Detection and Removal of Microplastics in Water Treatment: a Laboratory Evaluation

by

Meghan Lea

Submitted in partial fulfilment of the requirements

for the degree of Master of Applied Science

at

Dalhousie University

Halifax, Nova Scotia

April, 2023

Table of Contents

List of Tables

List of Figures

Abstract

Plastic production has significantly increased over the past 50 years due to its low cost, ease of production, versatility, and durability. Plastic materials take decades to degrade and could remain in the environment indefinitely. Once plastic is disposed of, it encounters several environmental elements that ultimately will break down these plastics into smaller fragments known as microplastics. These plastics may eventually find their way into a water treatment plant via numerous channels. Once these plastics enter the treatment system, a facility's ability to remove them relies on the treatment used.

This thesis investigates the presence of microplastic pollution in drinking water and wastewater treatment facilities and the efficiency of these facilities in removing microplastics using conventional treatment under varying influent turbidities. This study found that as raw water's turbidity increased, microplastic removal increased, indicating that influent turbidity may be an essential factor in removing microplastics in treatment facilities.

Additionally, the thesis explores using a UV-LED collimated beam to rapidly age microplastics in a lab setting. This method was validated through FTIR spectra comparison to environmental samples and SEM imaging, demonstrating its efficacy in aging microplastics for further study. These findings are significant because they contribute to a better understanding of the challenges of removing microplastics from water treatment facilities and provide insight into potential solutions for more effective removal.

Moreover, aged plastics performed better under conventional treatment than unaged plastics, indicating that the aging process may enhance the removal of microplastics from water treatment facilities. In addition, aged plastics were found to absorb more heavy metals than unaged plastics, suggesting that aged microplastics may play a role in transporting heavy metals in aquatic environments.

The study also underscores the importance of continued research in this area to ensure drinking water's safety and quality and protect the environment from the negative impacts of microplastic pollution.

List of Abbreviations

ATR - FTIR Spectroscopy

CI – Carbonyl Index

DLS - Dynamic Light Scattering

DOC – Dissolved organic carbon

DWTP – Drinking water treatment plant

EDS - Energy Dispersive X-ray-Spectroscopy

FFF - Field Flow Fractionation

HRM – Halifax regional municipality

JDKWSP - J.D. Kline Water Supply Plant

ICP-MS – Inductively coupled plasma mass spectrometry

MP – Microplastic

NOM – Natural organic matter

NTA - Nanoparticle Tracking Analysis

O_3 - Ozone

Pb – Lead

Pb^{2+} - Lead cation

PE – Polyethene

PS – Polystyrene

Py–GC/MS - Pyrolysis-Gas Chromatography Mass Spectrometry

SEC - Size Exclusion Chromatography

SEM - Scanning Electron Microscope

TEM - Transmission Electron Microscope

µg/L - Micrograms per litre

µm - Micrometers

UV -VIS Spectrophotometry

WWTP – Wastewater treatment plant

Acknowledgements

I would like to express my deepest gratitude to my thesis advisor Dr Graham Gagnon; your guidance and support have been invaluable throughout the research process. I learned more than I ever thought I could, and I am so grateful for my experience. Your expertise, encouragement, and patience have been instrumental in helping me to the finish line.

I would also like to thank my committee members, Dr Amina Stoddart and Dr Tony Walker, for their insightful feedback and valuable suggestions, which have contributed significantly to the quality of this work and generated many unique further research ideas.

I am grateful to the staff, students, and researchers at CWRS for their assistance and collaboration during my lab work. Their expertise and knowledge have provided me with the necessary resources and technical support for my research and helped me develop all my experiments. They all provided me with constant support and encouragement throughout this journey. Their enthusiasm, feedback, and advice have been instrumental in shaping my ideas and providing me with a fresh perspective.

Finally, I would like to thank my family for their unwavering love, support, and encouragement. Their understanding and patience have been instrumental in allowing me to pursue my academic goals and complete this thesis.

Chapter 1 Introduction

Over the past 50 years, worldwide plastic production has increased by over 300% (Geyer et al., 2017). It is forecasted to have a steady incline in output due to the minimal production costs, high durability, low weight and elasticity (Gourmelon, 2015). Currently, at least 45 different types of plastics are being produced for commercial use, all with differing chemical structures, toxicity levels and durability within the environment (Chamas et al., 2020). Many plastics are considered environmental pollutants as they biodegrade very slowly and can remain within the environment indefinitely (Yu et al., 2022).

An estimated 75,000 – 500,000 tons of microplastics (MPs), defined as water-insoluble, solid polymer particles that are smaller than 5 mm (Hwang et al., 2020), are released annually as either primary or secondary microplastics worldwide. Classification as either primary or secondary depends on their origins. Primary microplastics are intentionally manufactured to serve a function, such as exfoliant beads for hand soaps, toothpaste, and cleaning products (Hwang et al., 2020). Secondary microplastics are by-products of either mechanical, chemical, or biological degradation of plastic litter accumulated in the environment (Efimova et al., 2018). The primary sources of plastic contamination in water are surface run-off, wastewater effluent, as well as from combined sewer overflows, industrial effluent, degraded plastic waste and atmospheric deposition (Schernewski et al., 2020). Microplastics can accumulate in lakes, rivers, and oceans (Tofa et al., 2019) and impact ecological systems. Microplastics have been found within the epithelial tissue of fish (Atamanalp et al., 2021). A potential human health risk is the ingestion of plastic-contaminated seafood (Smith, 2018). Once ingested, microplastics can accumulate within the human digestive tract resulting in an increased risk of adverse health impacts, including digestive problems, reproductive system effects, and respiratory function problems

(Kurunthachalam, 2021). Evidence has shown that microplastics <20µm could penetrate a cell wall and accumulate within a cell, causing damage to the cell's DNA. Furthermore, additives in plastic products such as phthalates, bisphenol and organotins can cause thyroid hormone disruption and alter the production of adipogenous cells (Enyoh et al., 2020).

Preliminary investigations have confirmed that conventional primary treatment processes for both drinking water and wastewater can remove most of the MPs (> 90%) and large particles (> 10µm) due to settling and filtration (Lapointe et al., 2020; Mason et al., 2016; Zhang et al., 2020b). However, non-negligible amounts of small-sized MPs remain in the final effluent of drinking water treatment plants (DWTPs) and wastewater treatment plants (WWTPs). Considering that both municipal DWTPs/WWTPs produce large daily discharge volumes, it suggests that many MPs are still entering the distribution systems and exiting the receiving water bodies. Therefore, both DWTPs/WWTPs are seen as significant sources of MPs (Bretas Alvim et al., 2020; Ngo et al., 2019)

Once microplastics are in the environment, they can encounter different weathering agents that can cause them to break down or degrade over time. These weathering agents can significantly impact the fate and transport of MPs in the environment. This exposure may alter their specific surface areas and the functional groups located on the microplastic surface (Zhang et al., 2022). This may gradually reduce MPs' size, facilitating their mobility through natural and engineered systems (Li et al., 2018). Current lab trials primarily rely on results from pristine MPs containing little to no surface weathering. These results may not accurately depict how an MP would behave in the environment due to the degree of weathering.

MPs can be a vector for heavy metal transport within a water treatment system(Liu et al., 2021). When water containing microplastics and heavy metals enters a water treatment plant, the microplastics can be retained in the plant's filters and sedimentation basins. Heavy metals that are adsorbed to or concentrated on the surface of the microplastics can then be released into the treated water when the microplastics are removed from the filters or sedimentation basins (Chowdhury et al., 2016). In addition, the microplastics that the treatment plant does not retain can be discharged into the environment, where they can continue transporting heavy metals. This can lead to the spread of heavy metal contamination in both treated water and natural water bodies (Krishna et al., 2018). As a result, microplastics in water treatment systems can pose a risk to human health and the environment and highlights the importance of effective microplastic and heavy metal management in water treatment processes.

1.1 Objectives

These adverse issues have motivated research into new technologies for enhanced detection and removal of microplastics from known sources. Microplastics have been found at all levels in drinking water and wastewater treatment facilities, likely entering the treatment facility within the influent. The research questions for this thesis are:

1. What impact does UV irradiation have on microplastics?
    a. What methods can be used for quantifying aging?
    b. Would the use of a collimated beam be an appropriate rapid in-lab aging method for microplastics?
    c. Does this aging alter the adsorption capacity of microplastics when exposed to heavy metals?

2. What is the removal efficiency of microplastics from both drinking water and wastewater using coagulation/flocculation/sedimentation?
    a. What methods can be used for quantifying microplastics in water?
    b. How do increasing levels of influent turbidity impact removal?
    c. How does the addition of polymer in wastewater treatment affect removal?
    d. How does weathering affect their response to treatment?

1.2 Thesis Organization

Relevant background information on current microplastic removal, aging, adsorption capacities and detection methods are located in Chapter 2. Chapter 3 presents materials and methods for all experimental studies done. Chapter 4 examines the premise that microplastics behave differently based on changes in surface morphology and aims to provide an in-lab method for the aging of plastics. Chapter 5 compares both aged and pristine microplastics to determine how their removal efficiency changes along with changes in influent water quality. Chapter 6 examines the in-lab weathered microplastics in a batch adsorption experiment to assess the influence that both surface weathering and dissolved organic matter (DOM) would have on heavy metal adsorption capacity. Chapter 7 presents overall conclusions from the current work and recommendations for future studies for this work.

Chapter 2 Background

2.1 Occurrence of microplastics

Currently, in Canada, there are no governing regulations for minimum concentrations of microplastics within a water treatment system. California has implemented governing regulations in 2018 which monitor plastic concentrations of source water, becoming the first government in the world which has established health-based guidelines for acceptable levels of microplastics in drinking water (Coffin, 2023).

There are also no standardized methods for detection or removal. These limitations and the prevalence of plastic waste in the environment make microplastics an emerging contaminant of concern in drinking water.

Microplastics have been reported in all the world's oceans, including polar regions (Bergmann, 2022). Since microplastics have a relatively low density compared to seawater, they can rise to the surface or stay suspended within the marine environment (Wu et al., 2019). Microplastics were reported to be present in 96% of surface water samples taken from the Pacific Ocean and 100% of samples from surface water taken in the Mediterranean Sea (Cózar et al., 2014). This research shows a worldwide distribution of these MPs. Concentrations within ocean water samples have ranged from 0.34 particles/L to 102,000 particles/L (Wu et al., 2019). Though this range in values is large, areas with more MPs are often found near converging ocean currents where litter can accumulate and in areas close to large urban centers (Osorio et al., 2021).
The factors affecting the distribution include large-scale forces such as wind and ocean currents, turbulence, and climate change (Ballent et al., 2012; Turra et al., 2014). As critical factors, the

inherent properties of microplastics, such as density, shape, and size, can also affect transportation and distribution patterns (Eerkes-Medrano et al., 2015).

Freshwater sources such as rivers, lakes, and streams are essential drinking water sources and provide critical habitats for aquatic organisms. Unfortunately, these sources are also vulnerable to microplastic pollution for several reasons. Firstly, freshwater sources receive microplastics from various sources, including wastewater, stormwater run-off, agricultural run-off, and atmospheric deposition (Li et al., 2018). Microplastics can enter freshwater sources through these pathways and accumulate in sediment, water column, and marine life (Wagner et al., 2014). Microplastics are challenging to quantify in any water matrix due to their small size and the complexity of the environment.

The impacts of microplastic pollution on freshwater ecosystems are not fully understood, but studies suggest that they can significantly impact aquatic organisms (Wang & Wang, 2018). For example, microplastics can be ingested by small organisms such as plankton or krill, which can then be consumed by larger organisms (Botterell et al., 2019). This can lead to biomagnification, where the concentration of microplastics increases as it moves up the food chain. This can harm the health of fish and other aquatic organisms (Zhu et al., 2020)

Several studies have reported the worldwide occurrence of MPs in major lakes and rivers, often serving as drinking water sources for large populations (Li et al., 2018). The amount of microplastics in a freshwater source is variable and highly dependent on current urban development, waste management and hydrological conditions. Generally, areas with higher

populations would experience higher levels of MP contamination. These findings were corroborated by a study done in 2015 by Eerkes - Merano. This study showed high levels of MPs in the surface waters of Lake Erie, which is close to many densely populated city centers such as Cleveland and Buffalo. These levels were compared to surface water samples from Lake Superior, a larger lake with far fewer large population centers, and these samples contained far fewer MPs/L. The current knowledge on microplastic-related occurrence studies primarily is about ocean water and sediment contamination, with limited studies published being about freshwater sources (Peller et al., 2020)

Both wastewater and drinking water treatment plants have been shown to contribute significantly to MP occurrence within the environment. The most significant contributor to microplastic pollution in freshwater sources is wastewater treatment plants. Moreover, wastewater treatment plants are not designed to capture and remove microplastics precisely. This means that even if microplastics are removed from the wastewater during treatment, they will likely end up in the sludge produced by the treatment process. This sludge is often used as fertilizer or disposed of in landfills, which can release microplastics into the environment (Harley-Nyang et al., 2022).

The exact number of microplastics released by wastewater treatment plants each year is challenging to estimate due to various factors, including the size and capacity of the treatment plant, the type of treatment process used, and the sources and concentration of microplastics in the wastewater. Rochman et al. (2015) used data published data from Magnusson and Norén (2014) and Martin and Eizhvertina (2014) to estimate the number of microplastics being discharged into aquatic habitats within the USA. The model yielded a conservative estimate of 8

billion microplastics released from municipal WWTPs daily. Similarly, Mason et al. (2016) studied effluent samples of 17 major WWTPs to quantify the overall discharge values of microplastics. The predicted model yielded that the average discharge of microplastics from US municipal WWTPs was approximately 13 billion pieces per day. A study conducted in the United Kingdom estimated that around 6.3 million microplastic particles are released from a wastewater treatment plant each day (Harley-Nyang et al., 2022). Another study conducted in Australia estimated that a single wastewater treatment plant could release up to 4 billion microplastic particles daily (Ziajahromi et al., 2021).

Given that high volumes of treated and untreated wastewater are released globally, and only around 60% of municipal wastewater is treated (Mateo-Sagasta et al., 2015), a considerable amount of microplastics would enter the environment via the discharges from WWTPs. In addition, other sources such as surface run-off, atmospheric fallout (Dris et al., 2016) and direct waste disposal contribute to the increase of microplastics in an aqueous environment.

However, it is important to note that these estimates are based on a limited number of studies and may only be representative of some wastewater treatment plants. The actual amount of microplastics released by wastewater treatment plants could vary significantly depending on various factors.

Overall, while the exact number of microplastics released by wastewater treatment plants is uncertain, these facilities greatly contribute to microplastic pollution, and efforts should be made to minimize their impact. Strategies such as improving wastewater treatment processes, reducing

the use of microplastics in consumer products, and implementing more effective methods for microplastic removal from wastewater can help reduce the number of microplastics released by these plants.

2.2 Current Removal in Water Treatment

Once a microplastic has made its way through a water treatment facility, there are no longer any barriers to protect the end user. This plastic is susceptible to encountering any other contaminants that may be present within a distribution system.

To date, microplastics have been identified in tap water in over 94% of treated water sources in the United States (Kirstein, Gomiero, et al., 2021), meaning that currently employed treatment trains cannot remove all microplastics from the influent. Systems which receive influent from groundwater sources have been found to have far lower levels of microplastics than those that receive influent from surface water sources. This is due to environmental contamination and run-off observed in a surface watershed (Cherniak et al., 2022). A study conducted by Piconkonsky et al. in 2018 aimed to quantify the number of microplastics being removed through conventional drinking water treatment, to understand the amount, size and makeup of microplastics being introduced into the drinking water system (Pivokonsky et al., 2018). This study tested three drinking water treatment processes, all employing coagulation/flocculation with different filtering techniques. Treatment plants which used sedimentation, sand and granular activated carbon filtration after coagulation/flocculation yielded a maximum removal of 86% and a minimum removal of 75%. While the removal techniques employed could remove most of these

plastics, the remaining concentrations were not negligible. They implied that potable water might be an important source of microplastic contamination within humans. The size of these microplastics was primarily (<90%) under 10μm. Twelve different plastic materials were observed in the treated water samples, with polypropylene (PP) being the most abundant. The materials that followed in significant concentrations were polyethylene (PE) and polystyrene (PS) (Pivokonsky et al., 2018). Multiple studies have supported the finding that advanced drinking water treatment employing coagulation/flocculation followed by granular activated carbon filtration has yielded the highest removal of microplastics for treatment technologies being used in industry to date (Lapointe et al., 2020; Zhang et al., 2020b, 2021).

A water treatment facility's ability to remove microplastics depends on the technology used. The addition of coagulants aids in the removal of microplastics since these negatively charged particles coagulate and increase in size, making them easier to remove. Granular filtration can only remove plastic particles larger than 100 μm; anything smaller is likely to find its way into the treated water system unless finer filtration techniques are employed (Zhang et al., 2020b). Beyond size and surface chemistry, particle density is also influential. While dense microplastics (i.e., polyethylene terephthalate) may be better suited to removal by sedimentation processes, mid- to low-density microplastics (i.e., polyethylene, polypropylene, polystyrene) can be effectively removed with dissolved air flotation (DAF) (Ngo et al., 2019; Talvitie et al., 2017). This is due to the way that the sludge is removed in the two processes, where sedimentation removes sludge from the bottom of the tank, and DAF removes sludge from the top of the tank.

2.3 Factors Affecting Surface Morphology

When treatment plants fail to remove microplastics, following disinfection methods and environmental factors can contribute to further degradation and fragmentation of the remaining plastic particles. Previous work by Vibien et al. and Gill et al. in 2001 have shown that exposure to chlorine, O_3 and UV light are the driving factors in plastic degradation. Chlorine and O_3 can subsequently cause the inner surface of plastic pipes to oxidize. This can lead to cracking, reduced pipe lifetime, and fragmentation of a pipe's inner surface to leach into a distribution system (Vibien et al., 2001; Gill et al., 1999). In a distribution system, microplastics, both from the treated water and degraded from the distribution pipe surface, will interact with contaminants. Compared to pristine plastics, the adsorption of pollutants by degraded microplastics will be more complex due to the changes in surface characteristics (Boucher et al., 2015; Holmes et al., 2012; Li et al., 2021). Depending on water quality and treatment processes (e.g., corrosion control, disinfection), the surface charge, roughness, porosity, polarity, and hydrophobicity of microplastics can change.

Due to their high polymer nature, MPs are stable under conventional physical treatments, such as coagulation/flocculation and sedimentation. Contrarily, physiochemical processes, such as UV irradiation, have the potential to alter the surface of the MPs (Hüffer et al., 2018). UV irradiation is a widely used disinfection process employed by both wastewater and drinking water treatment facilities. This alteration to the MP's surface could affect how well it would respond to different treatment processes. Previous research has shown that the presence of suspended particulate matter such as MPs impacts the effectiveness of UV disinfection by reducing the amount of available energy for absorption for disinfection. These particles may also shield contaminants

located on the surface of the particle, shielding them from disinfection (Christensen & Linden, 2003).

Plastic degradation begins at the polymer surface, which is exposed to the environment and available for chemical attack (Gewert et al., 2015). Therefore, the degradation of a microplastic proceeds faster than meso- and macro-plastic, as microplastics have a higher surface-to-volume ratio. The first visual effects of polymer degradation are changes in colour and cracking of the surface. Surface cracking makes the inside of the plastic material available for further degradation, which eventually leads to embrittlement and disintegration.

MPs undergo aging in the environment, and the aging process mainly includes mechanical breakage, photo-degradation, thermal degradation, and biodegradation. The combined influence of various environmental factors on the MPs' aging process is complex, leading to unpredictable changes in the fate of MPs in the environment. UV light (sunlight) is seen as the most critical factor in the aging process of polymers since exposure is frequent within the natural environment (Ho et al., 2020). Understanding the impact of UV on the fragmentation and degradation process of all plastics is of great significance for further predicting the behaviour of MPs within the environment. The chemical oxidation induced by light is enhanced, showing a synergistic aging effect when multiple aging factors work together. Polymer photo-oxidation reaction generally includes four steps: chain initiation, chain growth, branch formation and chain termination (Gewert et al., 2015). The degradation of a polymer occurs when unsaturated structures or additives within the polymer absorb UV light to form free radicals. These free radicals form from

the breaking of C-H bonds which then interact with oxygen to generate more free radicals, which accelerate its aging (Gewert et al., 2015).

The term ageing of polymers is usually associated with long-term changes in polymer properties under the conditions of weathering and may involve any of the above processes.

In the case of polystyrene, when the polymer is irradiated from exposure to UV light, the phenyl ring becomes excited, and the excitation energy is emitted to the next C-H bond, breaking the bond. This transfer of energy causes the formation of free radicals within the polymer (Yousif & Haddad, 2013). End-chain scission is the predominant mechanism for degradation (vs random scission). Therefore, styrene monomers are the most abundant product of polystyrene degradation since chains are broken on either end. The further production of these monomers increases the rate of polymer degradation.

2.4 Adsorption mechanisms of heavy metals

In general, the adsorption mechanism between MPs and heavy metals can be described by electrostatic interactions, van der Waals forces, π–π interactions, pore filling, hydrogen bonding and hydrophobic interactions (Fu et al., 2020; Lin et al., 2021; Torres et al., 2021). The sorption behaviour of contaminants to MPs is dependent on solution chemistry. It was observed that polystyrene (PS) microparticles have an isoelectric point at a pH of around three, which implies that in the natural aqueous environment, these MPs should carry a negative surface charge (Lin et al., 2021). The electrostatic attraction between these negatively charged MPs and positively charged metal ions promotes adsorption. PS is negatively charged due to the presence of

carboxylic acid groups on the surface. Compared to electrostatic interactions, van der Waals forces, hydrogen bonding and π–π interactions play a relatively minor role (Fu et al., 2021). However, they can further promote the sorption capacity. Specifically for PS, π–π interactions are more present due to the increased number of aromatic structures present on the surface (Nguyen et al., 2022).

Electrostatic attraction simply refers to the attractive force that exists between positively and negatively charged particles. In the context of heavy metal adsorption to microplastics, electrostatic attraction plays an important role. Microplastics are often negatively charged due to the presence of functional groups on their surface, while heavy metals in water are typically positively charged. This creates an electrostatic attraction between the microplastic surface and heavy metal ions, leading to adsorption. The strength of the electrostatic attraction depends on the charge density and distribution of both the microplastic surface and heavy metal ions.

Van der Waals forces are described as a weak, short-ranged, electrostatic attraction due to a momentary change in polarity where one side of the molecule becomes much more electron-dense than the other. This electron-dense side now momentarily imparts a more negative charge and will have a higher affinity for cations present in the solution. This force arises from the dipole moment of the heavy metal ion and the induced dipole moment in the microplastic surface due to the presence of polar functional groups. These forces are highly reversible and could lead to the desorption of adsorbate within the solution (Tsuchiya, 2018).

π–π interactions, in terms of metal adsorption, occur between the electron-rich pi system present within an aromatic molecule. These electron-rich systems interact with the positively charged metal ion. These can also be described as pi–cation interactions. Several factors influence the strength of the bond: the nature of the cation, the nature of the π system, and the geometry of the interaction (Atugoda et al., 2021; Liu et al., 2021). In terms of strength, these interactions are stronger than Van der Waals since these are a type of covalent bond.

Hydrogen bonding is another weak electrostatic attraction which is described as a hydrogen atom located between a pair of atoms which have a high affinity for electrons; these bonds are weaker than an ionic bond or covalent bond but stronger than van der Waals forces. One atom is covalently bonded to a hydrogen atom, where the electron is shared unequally, giving the hydrogen side a more positive charge and the donor side a more negative charge. This more negative charge can cause the electrostatic attraction between cations to present within the solution (Vladilo & Hassanali, 2018).

Pore filling is an adsorption-like interaction. This is the process of contaminants becoming entrapped within the microscale pores of an MP. Pore filling is controlled by the diffusion of contaminants from the bulk phase to the surface of the MP. It has been found that microplastics which have been exposed to the environment contain a higher micropore area than that of virgin MPs, and the pore-filling sorption capacity is, therefore, higher for aged MPs.

Hydrophobic interactions can also play a role in the adsorption of lead onto polystyrene microplastics. Polystyrene is a hydrophobic material, meaning it repels water. Lead ions, on the

other hand, are hydrophilic and are surrounded by a layer of water molecules. When lead ions encounter the hydrophobic surface of polystyrene microplastics, they can be attracted to the surface through hydrophobic interactions (Faghihnejad & Zheng, 2013; Zhang et al., 2019). Adsorption kinetics refers to the rate at which heavy metals adsorb to microplastics over time. The kinetics of adsorption depends on several factors, including the concentration of heavy metals in the surrounding solution, the surface area and charge of the microplastics, and the nature of the heavy metal ions. Generally, the adsorption of heavy metals to microplastics follows a rapid initial stage, where many metal ions are adsorbed quickly, followed by a slower stage where adsorption slows down and eventually reaches equilibrium. The rate of adsorption can also depend on the size and shape of the microplastics, as well as the temperature and pH of the solution.

2.5 Previous work on heavy metal interactions

Multiple studies have been conducted to quantify the amount of heavy metal adsorption occurring due to microplastics within an aqueous solution (Liu et al., 2021; Nguyen et al., 2022). These studies, however, do not mimic environmental drinking water conditions as well as microplastic concentrations that would be observed in a treated water source. A study conducted by Ho et al. determined that the maximum uptake of Pb ions to a pristine microplastic occurs when the pH is increased. This is due to the intensified electrostatic attraction between microplastics and Pb at increased pH. These interactions are intensified due to microplastics (specifically polystyrene) having an isoelectric point around 3. For any pH higher than 3, the microplastics will exhibit a higher negative zeta potential.

A study conducted in 2020 aimed to investigate how changes in water constituents affected the adsorption rates of different metals (Cu, Fe, Pb, Mn, Zn) to microplastic surfaces, both aged and not-aged (Huang et al., 2020). This research concluded that the driving factors in metal adsorption for plastics were changes in pH and changes in the surface morphology of the plastic particles. As particles age, essential changes in surface morphology occur, where a greater number of adsorption sites are created, thus providing adsorption sites for metals and/or NOM.

To evaluate the interaction of plastic with metal ions in a simulated environmental context, experiments with variable levels of organic matter have been performed. Dissolved organic matter can adsorb to dissolved metals (Caprara et al., 2016; Martell et al., 1988; Plöger et al., 2005) and can therefore aid or inhibit metal adsorption onto microplastics. Organic matter in water can form complexes with metals and therefore lower the dissolved metal ions' activity within a solution, making them unavailable for adsorption to the plastic (Liu et al., 2020). Organic matter is also able to adsorb onto plastic, both through hydrophobic interactions and through weak interaction with charged functional groups located on the surface of the plastic. These interactions possibly enhance the accumulation of metals on the plastic surface by increasing the density of negative charges on the primed plastic and, consequently, an affinity for metal ions (Li et al., 2019).

Because of such complexity, earlier studies sometimes yielded contradictory results. For example, Tang et al. (2020) showed that fulvic acid in the solution negatively affected the adsorption of Pb onto aged nylon MPs, possibly due to the complexation between fulvic acid and Pb (forming dissolved Pb – NOM complexes). A similar behaviour was observed with humic

acid, competing with different microplastic polymers for Cd adsorption done by Zhou et al. (2020). Both studies indicate that organic matter would inhibit adsorption capacity onto microplastics due to the formation of NOM-metal ion complexes.

In contrast with these results, Fu et al. (2020) and Godoy et al. (2019) observed increased adsorption of Pb, Cr and Cu on different polymers in tap water and wastewater (compared to distilled water) and proposed that the interaction was enhanced by DOM present in these matrices by the organics creating a bridging effect between the microplastic surface and the heavy metals (Binda et al., 2021).

2.6 Methods to analyze MPs

Despite significant evidence of abundant microplastic waste within the environment, no standardized methods for sampling, extraction, analysis, evaluation, and classification of microplastics in aquatic samples exist. However, the variety of methods used has led to a wide range of data which makes comparison difficult due to the wide variability of data. Therefore, a harmonized detection approach is needed for future comparisons and for research to move forward. These discrepancies in methods can lead to an extensive range of data and the inability to compare results accurately.

The current techniques used can be classified into two types of identification: physical characteristics and chemical characteristics (Luo et al., 2022). Physical characteristics include size, shape, colour, crystallinity, and surface morphologies. In contrast, chemical characteristics cover elemental makeup, light absorption capacity, and present functional groups. The main

objective of this review is to describe analytic methods for the detection, characterization, and identification of MPs in different aquatic matrices. Among the analytical methods, chemical characterization techniques such as spectroscopy will be described, although some microscopic techniques, such as transmission electron microscope (TEM), scanning electron microscope (SEM), and fluorescence microscopy, have an analytical potential that allows for identifying and determining the chemical and physical properties of many polymers. The advantages and limitations of the different microscopic and analytical techniques will be discussed in Table 2-1.

Table 2-1 *Comparison of known commonly used methods for microplastic detection.*

Method	Size range	Detection Target	Advantages	Disadvantages	References
Visual Sorting (Optical Microscope)	<50 µm	Size, shape	Low cost Identification of size, shape, and colour	The polymer type of the samples cannot be determined and necessary to couple with identification methods listed below	(Prata et al., 2020), (Dris et al., 2017), (Chen et al., 2020)
SEM imaging	0.01 - 1 µm	Size, shape, qualitative analysis, morphology	The ability to show active binding/adsorption onto MPs show a visual of aging by showing changes in morphological structure When combined with EDS can	High cost Low maneuverability can only analyze a small segment of the sample at a time	(Cai et al., 2017)

			show elemental composition Can detect very small-sized particles		
ATR - FTIR Spectroscopy	50 - 500 µm	Chemical composition	Non-destructive, Large spectral library	Ambient air and humidity can severely impact readings A large enough volume of sample is needed to fully cover the detector Not quantitative	(Käppler et al., 2016),(Liu et al., 2019),(Luo et al., 2022),(Mani et al., 2015)
Raman Spectroscopy	1 – 50 µm	Chemical composition	Non-destructive Can detect additives	Not quantitative A large enough volume of sample is needed to fully cover the detector. Spectra library is not as broad as FTIR	(Käppler et al., 2016),(Klein & Fischer, 2019)
Membrane filtration with weighing	0.01 - 12µm (pore size dependent)	Concentration, discrete size range	Ease of use Minimal sample preparation Large variety of filter media and pore size	Time-consuming Large sample volume required Low size selectivity	(Mausra & Foster, n.d.), (Möller et al., 2020)

				(pore size and higher)	
Field Flow Fractionation	0.001 – 1μm	Size Distribution, hydrodynamic radius	Provides continuous size distribution High resolution with continuous particle separation	Long setup times High sample dilution occurs during sample migration in the channel to the detector, which limits the mass sensitivity Analytes can interact with the chamber wall and membrane, which could give low particle recovery	(Fu et al., 2020),(Contado, 2017; Mintenig et al., 2018)
UV -VIS Spectrophotometry	--	Concentration	Easy to setup, quick readings	Calibration curve needed for each new influent High analyte concentrations needed for detection Not suitable for environmental samples	(Hofman-Caris et al., 2022),(Fan et al., 2022)
Dynamic Light Scattering (DLS)	0.006 - 10μm	Bulk size distribution Hydrodynamic Diameter	Minimal Sample prep Easy to use, quick readings	Low resolution Not suitable for samples where settling occurs, low concentrations or aggregation,	(Boyd et al., 2011),

				or polydisperse samples Large particles may block smaller ones, skewing size range	
Nanoparticle Tracking Analysis (NTA)	0.01 – 2µm	Concentration, hydrodynamic radius	Can detect individual particles and aggregates	High cost Does not provide imaging or morphology	(Boyd et al., 2011),(Karimi Estahbanati et al., 2023, p. 5)
Transmission Electron Microscope (TEM)	0.001 – 1µm	Size, shape, qualitative analysis, morphology	Able to capture nanosized particles Minimal sample preparation Both wet and dry samples can be used	High cost, Low maneuverability Unable to analyze large number of samples	(Sun et al., 2018)
Size Exclusion Chromatography (SEC)	0.001 – 1µm	Size, effective radius	Minimal sample volume needed Non-destructive	Analytes can interact with the chamber wall, which could give low particle recovery Calibration curve standard needed	(Biale et al., 2021)
Pyrolysis-Gas Chromatography Mass Spectrometry (Py–GC/MS)	>100 µm	Chemical composition, size distribution	Can separate sample from contaminants based on size and polarity	Require larger particle masses compared to vibrational microscopy-	(Kirstein, Hensel, et al., 2021),(Peters et al.,

				orientated methods. Destructive to sample Method for microplastic detection not well studied	2018),(Hermabessiere et al., 2018)

2.6.1 Visual Sorting

This method uses an optical microscope to separate individual microplastics from one another/from the sample. If large plastics (> 5mm) are the target area of study, then visual sorting and inspection can be done without a microscope, as these are no longer considered microplastics. If particles are smaller (< 5mm), then a microscopic technique should be employed to aid in visual sorting (Löder & Gerdts, 2015). This method characterizes microplastics using size, colour, shape, and number of microplastics within a sample. This is a low-cost method that takes little to no sample prep.

One limitation of visual sorting is the inability to differentiate organic and inorganic matter from the microplastic samples. For instance, it is challenging to distinguish microplastics which are similar in colour to the sample background, making bright/opaque colours easier to identify than muted transparent ones. This can cause a large margin of error in counting and determining microplastic concentrations. Therefore, it is not recommended to use only visual observation for microplastics less than 500 μm (Hidalgo-Ruz et al., 2012).

2.6.2 Scanning electron microscopy

Scanning electron microscopy is a microscopic technique able to provide information about the morphological surface structure of MPs, generating high-resolution images of the surface state. If equipped with Energy Dispersive X-ray-Spectroscopy (EDS), it can also provide data about the chemical composition of the samples.

The electron microscope works by using a beam of electrons to form an image. The primary electrons penetrate the solid specimen, and both elastic and inelastic scattering processes are generated. The electron beam hits the atoms of the specimen, and those atoms absorb the energy and give off their electrons. A detector picks up these electrons, which form an image (Omidi et al., 2017).

The disadvantages of using SEM imaging are that samples must be conductively coated to obtain a reading (destructive to the sample), and this is a costly and time-consuming method. This method also has little maneuverability since it is only able to analyze small portions of a sample at a time and would not be helpful for samples having a large volume of microplastics. On the other hand, SEM imaging is easily able to show a degree of degradation of samples as indicated by changes in surface characteristics/morphology as well as if any contaminants have been adsorbed onto the plastic surface.

2.6.3 Transmission Electron microscopy

Transmission Electron microscopy can examine samples of nano sizes by using specific wave properties of electrons to gain a higher-resolution image (Goldstein et al., 2017). The main difference between SEM and TEM is that SEM provides an image by using reflected electrons,

while TEM uses electrons that pass through the sample (transmitted) to create an image. This allows the TEM to provide more information on the inner structures and crystalline structures of a specimen. TEM samples need to be very thin (< 150nm) so that the electron beam can entirely pass through the sample (Malatesta, 2021). TEM also requires complex sample preparation, such as electropolishing, mechanical polishing, and focused ion beam milling, before samples can be analyzed (Malatesta, 2021).

Dependent on what information is needed, either TEM or SEM would be used. In the case of microplastics, if the information needed regarded surface morphologies and/or contaminant adsorption detection, then SEM would be used. If the information needed was regarding crystal structure or structural defects, then TEM would be used.

2.6.4 Vibrational spectroscopy

The most common analytical methods used to identify microplastics in aquatic samples are Fourier transform infrared spectroscopy (FTIR) and Raman. Both vibrational spectroscopic techniques can characterize synthetic organic polymers and their products through a comparison of wavelength spectra. In vibrational spectroscopy, molecule vibrations of a sample are excited and detected, which leads to characteristic spectral fingerprints in the FTIR or Raman spectra (Chen et al., 2020). Thus, a characterization based on the polymeric chemical structure and identification by comparison with known reference spectra becomes possible.

Raman

Raman spectroscopy is a technique based on the interaction between radiation and material. This technique uses intense light from a laser that interacts with the chemical bonds of a substance,

which generates the re-emission of light at the specific wavelengths that are characteristic of the specific atomic groups. A Raman spectrum is therefore generated by the scattering between the photons of incident radiation and the molecules in the sample (Huppertsberg & Knepper, 2018). This technique works like FTIR analysis and has a minimum limit of detection of 1μm. This technique can be used to authenticate materials and/or determine chemical changes within a sample. The disadvantages of vibrational spectroscopy are that it is difficult to analyze samples containing many polymers or environmental samples since it is difficult to isolate individual materials.

Attenuated Total Reflection – Fourier Transform Infrared Spectroscopy (ATR - FTIR)

Using ATR - FTIR spectroscopy, the sample is irradiated with IR light (wavenumber range 400–4000 cm^{-1}). A part of the IR radiation is absorbed depending on the molecular structure of the sample and measured reflection model (Wang & Wang, 2018). Different samples have different compositions, resulting in different spectral images. By comparing the spectral images of samples with known materials in libraries, the type of polymer composing the microplastics can be identified. Compared with visual analysis, FTIR can analyze particles of small size, and the results of the identification are more reliable than only using one method.

The difference between the two methods is that FTIR measures how much light is remaining from the original light source after it is passed through the substance; any light that does not remain is assumed to be absorbed by the bonds within the sample. Raman, on the other hand, measures the light energy that is scattered after the sample has been excited by the laser (Exline, 2013). These two methods can complement one another to better determine what a substance is

comprised of. For example, Kappler et al. (2016) concluded that a particle whose Raman spectrum matched that of TiO_2 but whose FTIR spectrum matched that of acrylic resin was acrylic resin coloured with pigments containing TiO_2 (Käppler et al., 2016). This shows that the use of both methods together can give a more accurate representation of samples, especially when samples contain multiple materials.

2.6.5 Membrane filtration

Membrane filtration is the most common type of size separation method and is widely used across the water treatment industry. This method relies on the physical separation of colloids from the aqueous solution by passing through a membrane with a fixed pore size. In the case of detection, filtration is meant to be coupled with numerous other analytical methods to better determine microplastic characteristics. Membrane filtration can go down to the nano size (0.0005–0.001 μm), though membranes this size are expensive and time-consuming to use, dependent on sample volume. Furthermore, membrane filtration does not provide finite size distribution; instead, it is only based on the pore size (Quinn et al., 2017). Membranes sized at 0.45μm are most used in drinking water applications and determine the threshold size of a colloid being considered as dissolved (Wang et al., 2017). Membrane filtration is subject to many errors through filter media, filtering techniques, influent quality, and analyte adsorption onto the membrane.

2.6.6 Field flow fractionation (FFF)

This technique works by separating colloids based on size using a cross-flow perpendicular to the main parabolic flow, which separates colloids based on their mobility against the cross flow.

This technique is designed for the fractionation of colloids and particles. A concentration profile is created from the membrane depending on the cross-flow (Okada, 2007): smaller particles diffuse further into the channel than larger particles based on mobility. The advantage of using FFF for microplastic detection is that a continuous size range of colloids can be determined within a relatively short period. Coupled with Inductively Coupled Plasma Mass Spectroscopy (ICP-MS), this method could indicate if metals are binding to the surface of colloids within a solution. Disadvantages of this method are the lengthy setup times as well as the current lack of knowledge for detecting polymers within an environmental solution, as well as limited detectors available that are specific for identifying plastics.

2.6.7 Dynamic Light Scattering (DLS)

Basic operations of light scattering methods require little operator training and measure the bulk sample size distribution of samples. DLS works by measuring the hydrodynamic diameter of particles as a factor of Brownian motion, and this motion is related to particle size. Light scattering cannot distinguish between individual particles and agglomerates or between particles of different compositions, nor can it provide information on the chemical composition (Boyd et al., 2011; Stetefeld et al., 2016). DLS provides low-accuracy measurement due to the low resolution of large aggregates and settling. As well, measurements can be skewed when sample concentrations are too low, or particles are too small.

2.6.8 Nanoparticle Tracking analysis (NTA)

Nanoparticle Tracking analysis is a visualization method for analyzing particles in a solution relative to the Brownian motion of the particle. A particle can be measured individually using a light-scattering laser and an ultramicroscope. The light that is scattered by the particles is captured using a coupled charge device (CCD) camera over multiple frames. This movement of particles is tracked frame by frame. The rate of the particles' movement is dependent on the sphere-equivalent hydrodynamic radius, which is calculated using the Stokes-Einstein equation. The advantages of this method are the minimal sample preparation, small sample volumes are needed, and samples can be analyzed in solution. Disadvantages of this method include the high cost and limited availability of this device, as well as the inability to show surface morphology (Boyd et al., 2011).

2.6.9 UV-VIS Spectroscopy

As a type of absorption spectroscopy, UV Spectroscopy is concerned with how molecules absorb radiation. Data is generated by directing UV light toward a sample. This excites the electrons within the sample and forces them to move from their ground state to a higher energy level (Tom, 2021). As this occurs, the electrons release wavelengths, also known as a spectrum. These patterns are used to determine the elemental composition of the sample. The detector then measures the amount of light absorbed by the sample at the specific wavelength. For concentration values to be determined using this method, the specific wavelength of the analyte needs to be known, and a calibration curve needs to be made at known concentrations. This method is only viable for a sample with a known analyte; environmental samples cannot be analyzed (Hofman-Caris et al., 2022).

2.6.10 Size Exclusion Chromatography (SEC)

Size Exclusion Chromatography (SEC), which is also called gel filtration chromatography, separates particles based on size by filtration through a gel located in a column. This gel contains porous spherical beads, and separation occurs when larger particles are unable to diffuse into these pores. This method can give a size distribution due to smaller particles having a longer residence time in the column since they are entrapped in the column. The advantages of this method are that separation can be achieved with minimal sample volume and can provide well-defined size separation of analytes. The disadvantages of this method are that particles could interact with the column walls, which would skew measurements(Patil, 2020).

2.6.11 Pyrolysis-Gas Chromatography Mass Spectrometry (Py–GC/MS)

This method works by breaking down a sample into smaller stable fragments through controlled thermal degradation (pyrolysis). This method can give both qualitative and quantitative measurements in samples. The coupling of pyrolysis with GC-MS allows for the elimination of sample extraction and dilution and can effectively analyze environmental samples. After the sample has been broken down, the mobile phase is used to separate the components, which are detected using mass spectrometry. This method is an appropriate tool for microplastic polymer identification and can give both qualitative and quantitative measurements. However, this method is constrained by sample size, as samples sized less than 10 μg are not easily detected, as well as the long sample preparation time (Peters et al., 2018).

Chapter 3 Materials and Methods

Sections 3.1 to 3.3 were employed for all lab work conducted throughout the study.

3.1 Glassware Preparation

All glassware was soaked for 24 hrs in a 10% nitric acid (HNO_3) solution. The glassware was then rinsed with de-ionized water four times and ultrapure water (MilliQ) four times and dried. This was done to ensure no metals or natural organic matter would remain on the glassware and impede readings.

3.2 Dissolved Organic Carbon (DOC) Analysis

Natural organic matter was measured as dissolved organic carbon. Samples were filtered through a 0.45 μm cellulose nitrate filter (Watman) and collected in a 40 mL vial with no headspace and acid preserved using 85% H_3PO_4.

3.3 Zeta Potential

The Zeta potential of all samples was taken on the Malvern Zetasizer. This measurement is the magnitude of the electric charge present between particles. Zeta potential was taken for all samples at all time points, including before and after experiments, to determine the overall change in electric charge.

3.4 In-lab aging of microplastics

3.4.1 UV Irradiation method

To simulate the emittance of a treatment process UV light, a UV- C LED collimated beam employing medium pressure lamps was employed. UV experiments were conducted using 280

nm wavelength, and irradiance was measured using a USB4000 Ocean Optics spectroradiometer (Ontiveros et al., 2021). The microplastics were placed in an 8-cm circular dish and placed 1.5 - cm below the beam. The average irradiance delivered to the samples was calculated to be 668 µW cm 2. UV irradiance dosages used were chosen based on a study completed in 2020, which used a minimum and maximum irradiance dosage of 180 mJ/cm2 and 3060 mJ/cm2, respectively (Lin et al., 2020). The maximum dose was set to 20 times the minimum dose to further the visual degradation of the samples. In practice, 186 mJ/cm2 is the UV dose required for virus inactivation according to the USEPA, meaning that surface waters in the US will receive this dose as the UV dose for treatment (Yates et al., 2006).

It should be noted that the setup of using a solution placed in a dish underneath the collimated beam is not a full representation of the type of UV inactivation that would occur. In a full-scale plant, disinfection would be achieved with irradiance from 360 degrees. An experimental design table can be seen below. Irradiation time was calculated using equation 1 below.

Table 3-1 *Irradiation dose and times for in-lab aging experimental setup.*

Irradiation Dosage (mJ/cm^2)	**Irradiation Time (min)**
180	4.54
1080	18.10
3060	43.43

$$\boldsymbol{Irradiation\ Time}\ [\boldsymbol{s}] = \frac{\boldsymbol{Irradiation\ Dose}\ [\frac{J}{cm^2}]}{\boldsymbol{Measured\ Irradiance}[\frac{W}{cm^2}]} \quad \textbf{(1)}$$

Irradiance was measured using a spectroradiometer, which indicates how much radiance is being emitted from a source.

Before irradiation, MPs particles were added to MilliQ and sonicated for 10 minutes to ensure a homogenous mixture. A volume of 30 mL of 1050 mg of MPs/L stock solution was added to a glass petri dish located 1.5 cm below the beam, and a stir bar was used to ensure particles were always moving throughout the exposure. A diagram of the setup can be seen below in Figure 3-1.

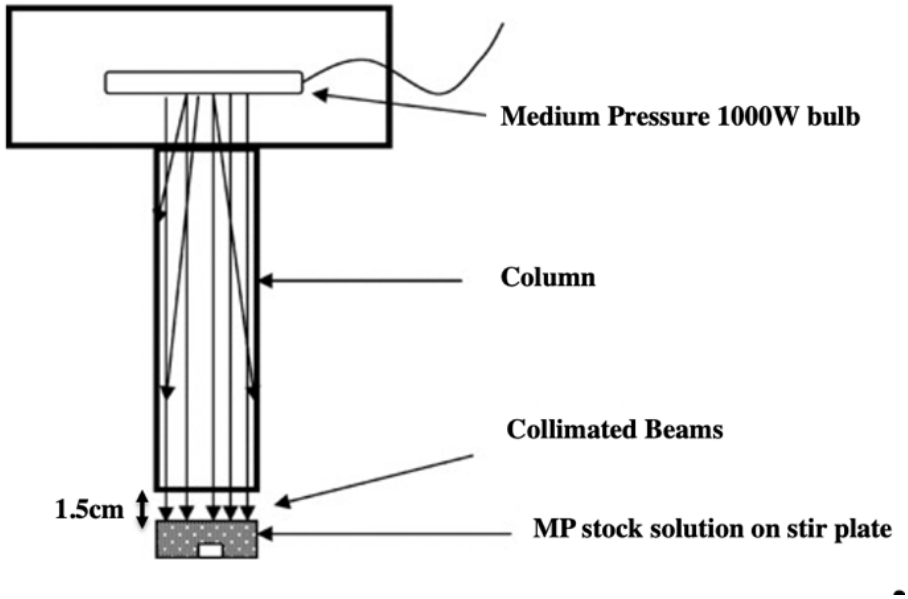

Figure 3-1 *Schematic of collimated beam setup*

Once the allotted irradiance time was reached, samples were syringe filtered through a 0.22 µm polycarbonate filter and dried for 48 hours in a desiccator. Control groups were conducted using the same MPs immersed in ultrapure water without UV treatment. The zeta potential was taken before and after irradiation; methods for this can be found in section 3.3.

3.4.2 FTIR Analysis

Samples were filtered through a 0.22 µm polycarbonate filter and dried for 48 before analysis to remove any water signals from analyzing a wet sample. A blank filter media (polycarbonate) was analyzed and used for spectrum subtraction to isolate the microplastic spectrum. Fourier

transform infrared (FTIR) spectroscopy was recorded using an Alpha II compact FT-IR spectrometer between 4000–400 cm^{-1}. This was used to identify the surface chemical characteristics of each sample and monitor changes within the absorbance.

3.4.3 SEM Imaging

Samples were prepared for SEM analysis by drying the filter material (polycarbonate) for 48 hours; once enough sample volume had passed, and the filter was coated with polystyrene. These filter samples were then cut and placed on SEM stubs and held in place using carbon tape since the carbon conducts an electrical charge allowing for SEM analysis to take place. The sample was then gold coated using a sputter coating device to further the electrical conductivity of the sample.

3.4.4 Image J Analysis

Using ImageJ (ImageJ, n.d.) analysis tool, surface measurements of microplastics were quantified with roundness, perimeter, and area. ImageJ was able to determine the area and perimeter of particles in SEM imaging, and from that, roundness was calculated using equation 2. 2.

$$\textbf{Roundness} = 4\pi\left(\frac{\textbf{Area}}{\textbf{Perimeter}^2}\right) \qquad (2)$$

3.5 Microplastic concentration detection method: UV-VIS Spectrometry

Calibration curves for both raw and treated water were created by spiking samples with known concentrations of microplastics and taking single wavelength readings at 290nm. A wavelength scan was done using a HACH DR6000 spectrophotometer, with a sample containing only MilliQ

and 1050 mg/L of polystyrene beads. This wavelength scan showed a significant absorbance spike at 290 nm and was therefore used to detect polystyrene. These wavelength spectra can be found in Appendix A. This value corresponds to many other studies quantifying PS using spectrophotometry for detection (Abedi et al., 2019; Li et al., 1991; Nurmukhametov et al., 2006)

The samples were spiked and measured at 0,2,4,6,8,10 mg/L of microplastics creating a six-point calibration curve. These concentration values are higher than environmental concentrations, but they were chosen to ensure a significant shift in absorbance was observed. These calibration curves were made for every influent as well as every treated sample every time samples were taken to ensure that influent variability was accounted for. The calibration from the raw water samples was only used to determine the recovery efficiency of the slope equation, while the treated water calibrations were used to determine removal efficiency. Using Beers Law, the absorptive capacity of the PS is directly proportional to its concentration in a solution. Using the slope of the line created through the calibration curve, absorption values from the spiked samples and the corresponding absorption value was plugged into the slope equation to determine the remaining microplastic concentration. Once the concentration values had been determined using the slope and intercept, the removal efficiency was calculated.

The removal efficiency was calculated by comparing the initial calculated value for concentration and comparing that to the calculated value for concentration after 40 minutes using equation 3:

$$\boldsymbol{MP\ removal}\ \% = \frac{\boldsymbol{Initial\ Concentration - Final\ Concentration}}{\boldsymbol{Initial\ Concentration}} \times \mathbf{100}\% \quad \textbf{(3)}$$

3.6 Jar Testing

Four replicates of each jar test were done at varying influent turbidities and duplicates of all measurements. Zeta potential was taken for all samples during all time stamps to determine how the overall charge of the solution was being affected, methodology for this can be found in section 3.3. Organic matter was measured by analyzing the amount of dissolved organic carbon (DOC) that was present in the sample; the methodology can be found in section 3.2.

3.6.1 Raw Water Characterization

Pockwock Lake is the surface water in which JDKWSP draws source water for treatment and is used as raw water for all experiments. This protected watershed is not influenced by industrial and/or treated wastewater discharge. Pockwock Lake is characterized by low turbidity, low alkalinity, and moderate NOM source water with a slightly acidic pH. This study was performed during July and August of 2022. Raw water characteristic ranges are presented in Table 3-2

Table 3-2 *Raw water characteristics.*

Measurement	**Range**
pH	5.5 – 5.9
Turbidity (NTU)	0.74 – 2.44
DOC (mg/L)	2.89 – 3.84

3.6.2 Raw Water Jar test protocols

Jar tests were conducted using raw water samples from Pockwock Lake, which supplies Halifax Water's largest drinking water treatment facility that supplies the city of Halifax, NS. The

turbidity of the raw water samples ranged from 0.7 NTU to 2.44 NTU. Two litres of influent were used for each jar, and the dosage of microplastics was 10 mg/L. The concentration of 10mg/L used was approximately 270 times smaller than the concentration used in a similar MP experiment through removal with coagulation/flocculation (Larue et al., 2003).

Two blank samples were used (one without plastics and one without coagulant), and two were dosed with microplastics and coagulant for replicate data. The coagulant used was aluminum sulfate at a dose of 18.5 mg/L, and the pH was increased to 6 by adding lime. The coagulant dosage and pH used for this study were based on the current dosages at the treatment facility. In drinking water treatment, a coagulant is dosed based on achieving turbidity levels < 1NTU. The raw water was equilibrated at 22°C for 10 seconds before experimenting. A volume of 19 mL of the microplastic stock solution was added (~ 19mL @ $6.7x10^{11}$ particles/L). This concentration is above environmental concentrations but was chosen to be able to detect microplastics using analytical tools. After adding lime, coagulant, and microplastics, the stirring speed was maintained at 142 rpm/min for 1 min and then decreased to 37 rpm/min for 12.5 min, 26 rpm/min for 12.5 minutes and 18 rpm/min for 12.5 minutes. There was also a subsequent 40 min sedimentation taking aliquots of the supernatant every 10 minutes. Each supernatant sample was analyzed using the HACH DR6000 Benchtop Spectrophotometer.

3.6.3 Wastewater Characterization

The influent being received by the DWWTF comes from a combined sewer system, meaning both municipal waste and road runoff are present in the influent. This makes treatment difficult as turbidity and influent characteristics are highly variable due to variability in the level of

stormwater dilution. The study was performed in July and August of 2022, taking samples from days where consecutive heavy rainfall occurred and days that were consecutively dry and hot. Influent characteristics observed throughout the experiment are reported in Table 3-3.

Table 3-3 *Wastewater influent characteristics.*

Measurement	**Range**
pH	6.5 – 7.2
Turbidity (NTU)	60.45 – 260.18
Temperature (°C)	11.5– 13.7

3.6.4 Wastewater Jar testing Protocols

Jar tests were conducted using post-grit influent water samples from the Dartmouth sewage treatment facility. The turbidity of the influent samples ranged from 60 NTU to 260 NTU. Two litres of influent were used for each jar, and the dosage of microplastics was 10mg/L. Two blank samples were used (one without plastics and one without coagulant), and three were dosed with microplastics and coagulant for replicate data. At the same time, one contained only coagulant and no polymer. The raw water was equilibrated at 22°C for 10 seconds before experimenting. A volume of 19 mL of the microplastic stock solution was added (~ 19 mL @ $6.7x10^{11}$ particles/L). This concentration is above environmental concentrations but was chosen to be able to detect microplastics using analytical tools. The coagulant used was aluminum sulfate at a dose of 9 mg/L, and the polymer dosage was 1.3mg/L. The stirring speed was maintained at 150 rpm/min for 1 min; the polymer was added and stirred for an additional minute at 150 rpm. The flocculation phase was held at 50 rpm/min for 10 minutes, followed by a 40-min sedimentation

phase, taking aliquots of the supernatant every 10 minutes. Each supernatant sample was analyzed using the HACH DR6000 Benchtop Spectrophotometer.

3.7 Batch Adsorption Experiment

To create synthetic water, two samples of 100 mL of MilliQ were dosed with 30µL of $NaHCO_3$ stock solution, and one was dosed with 100 µL of a 1g/L humic acid (HA) isolate as the surrogate for NOM. $NaHCO_3$ was used as a buffer to ensure pH levels stayed consistent. $Pb(NO_3)$ was added to the solution and, once the pH was stable, was brought up to 6 ± 0.2 by adding 0.1 M NaOH. 40 mL jars were rinsed using MilliQ and filled with duplicates of each solution. Two samples containing raw water, which had also been pH adjusted to 6 ± 0.2 by adding 0.1 M NaOH, were used for analysis, with an additional sample containing no plastics that would act as blank for control purposes. Losses to glassware, filtration apparatus and any precipitation of the lead were accounted for by having these blank samples for each water matrix. These blank samples were dosed the same way as all the other samples, without adding microplastics, to better isolate how much lead was being adsorbed to the MPs vs how much lead was being adsorbed by other surfaces.

The microplastics used for this experiment were 0.3 µm suspended polystyrene beads (Sigma Aldrich, LB3). The stock solution had a concentration of 1.05 g/mL of polystyrene; volume calculations for this can be found in Appendix A. The aged plastics have been weathered using 3060 mJ/cm^2 of energy using UV irradiation. More information on how these plastics were weathered can be found in section 4.2.1. All nine jars were sealed and placed on the shaker table

for 24 hours at 150 rpm. Initial measurements for dissolved organic carbon and total metals were taken from each sample.

3.7.1 Lead Analysis

Lead concentrations were analyzed using an inductively coupled plasma mass spectrometer (ICP-MS) (X series 2 ICP-MS, Thermo Fisher Scientific, MA, USA). 2 mL filtered aliquots from each sample were taken and diluted using 8ml of MilliQ to make a 10 mL sample. It was assumed losses to the filter media were negligible in comparison to solution concentrations, and losses were the same across all water matrices. These samples were treated with nitric acid for inductively coupled plasma mass spectrometry (ICP-MS) for filtered analysis and tested for total lead concentrations. The samples analyzed had a much greater lead concentration than the minimum detection limit of 0.4 µg/L of lead.

Adsorption experiments were conducted by adding two mg/L of Pb^{2+} to 100 mL of the synthetic water with an initial PS concentration of 1 mg/L and an initial DOM concentration of 1mg/L. The concentration of metal ions before and after equilibrium adsorption was determined using the inductively coupled plasma mass spectrometer (ICP-MS). The uptake value of metal ions at each time stamp was calculated according to equation 4:

$$q_t = \frac{(C_o - C_t)}{m} \cdot V \qquad (4)$$

Where m is the mass of the MPs (mg), and V is the volume of solution (L). C_o and C_t are the initial and final concentrations of ions (mg/L), respectively. C_o was found by using the metal concentration values for samples containing no plastics at each respective time stamp, performed

in sequence with the other jars. This was done to determine losses of metals attributed to adsorption to the glassware, filter media.

Chapter 4 IN-LAB AGING METHOD FOR ARTIFICIAL WEATHERING OF MICROPLASTICS

4.1 Introduction

Current studies utilizing microplastics primarily use pristine microplastics, which would not accurately represent how a microplastic would react within the environment. Aging causes changes in surface morphology and functional groups of a microplastic and, therefore, would impact how it would respond to treatment. Current in-lab aging methods span weeks to years, and no standardized method is used to quantify the amount of aging that has occurred.

The primary objective of this study aims to investigate the degree of degradation that polystyrene microplastics undergo when exposed to increasing amounts of UV irradiation and to determine if this is an appropriate rapid in-lab method for aging microplastics. Two different quantification methods were used to achieve these: changes in carbonyl indices and visual inspection.

4.2 Results

4.2.1 FTIR Analysis

Irradiation dose was set in the range of 180–3600 mJ/cm^2 to evaluate the surface chemical feature variations. FTIR was used to measure absorbance spectra to verify changes in chemical characteristics. As shown in Fig. 4-1, the FTIR spectra revealed new absorption peaks that appeared at 1670 cm ^{1}, which were identified as the characteristic peaks representing the stretching vibration of carbonyl groups (Carlier et al., 1986). These new peaks suggested the generation of carbonyl structures during UV treatment, even under the minimum irradiation dose of 180 mJ/cm$^{2.}$

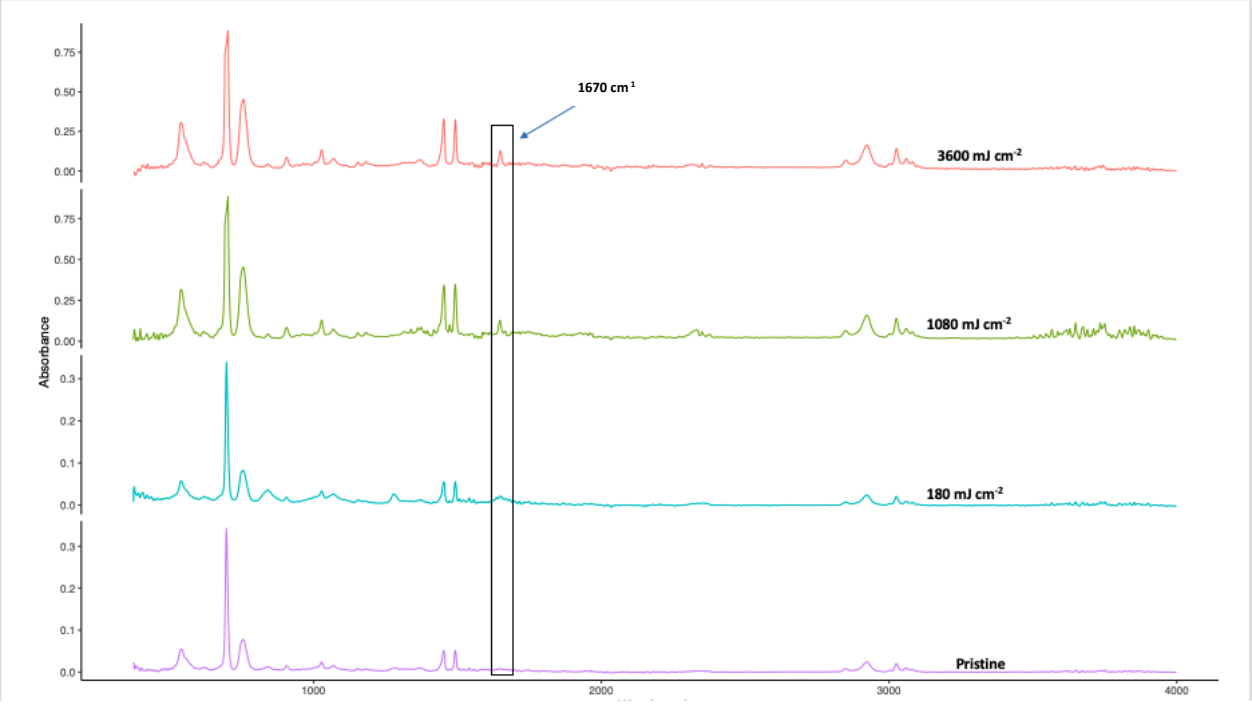

Figure 4-1 *FTIR Spectra for polystyrene exposed to increased levels of energy.*

The changes in the IR spectra indicate changes in functional groups on the plastics surfaces are occurring. Despite spectrum subtraction being used, peaks from the polycarbonate filter can still be seen around the 2500 band, which was determined by overlaying the filter spectrum on the treated particle spectrum. These spectrums can be seen in Appendix A. These peaks are not indicative of any changes to the MP surface, and a full FTIR spectrum of the filter can be found in Appendix A. The zeta potential of all samples was taken after each irradiation was completed. The zeta potential value remained consistent for all UV doses at -37 mV, which can be seen in appendix A, meaning that UV irradiation has no impact on the overall surface charge of the particles, only on their physiochemical structure. The weak alteration of the FTIR spectra is probably attributed to the unique anti-aging properties of polystyrene, such as UV stabilizers (Arangdad et al., 2019). Overall, the FTIR spectra obtained using the aging procedure in this

study compares well with recent reports on polystyrene MPs occurring in environmental samples, which also showed peaks around the 1670 cm^{-1} band (Mattsson et al., 2021; Sarkar et al., 2021). This demonstrates that this method of UV irradiation could be a viable option for in-lab weathering for the simulation of environmental microplastics.

4.2.2 Carbonyl Indices (CI)

A carbonyl index is a measurement used in analytical chemistry to quantify the degree of oxidation of organic compounds containing carbonyl functional groups. A carbonyl group is a functional group consisting of a carbon atom double bonded to an oxygen atom. The carbonyl index is calculated as the ratio of the absorbance at a specific infrared wavelength corresponding to the carbonyl group to the absorbance at a reference wavelength that is not affected by the carbonyl group. The higher the carbonyl index, the greater the degree of oxidation of the organic compound (Carlier et al., 1986). Currently, there is no standardized reference wavelength or method used for polystyrene.

Four different methods were used to determine carbonyl indices, which can be found in Table 4-1.

Table 4-1 *Carbonyl index calculation methods and their corresponding features.*

Method	Methodology	Specified Wavenumbers (cm^{1})	Range of CI Values	References
1	Ratio of maximum absorbance height	1670/2925	0.3 – 0.9	(Ville, 2015)
2	Average absorbance area of carbonyl peak over reference area reference peak	1625 - 1700/ 2900 - 2975	1.0 - 2.1	(Almond et al., 2020)
3	Ratio of maximum absorbance height	1670/1450	0.1 – 0.4	(Yousif & Haddad, 2013)
4	Average absorbance area of carbonyl peak over reference area reference peak	1625 - 1700/1425 - 1500	1 – 2.3	(Almond et al., 2020)

Methods 1 and 3 used the ratio of maximum peak values of two different reference peaks compared to the maximum absorbance peak in the carbonyl range (Ville, 2015; Yousif & Haddad, 2013), while methods 2 and 4 used the same maximum peaks but used the of the area under the curve for ratio comparison (Almond et al., 2020). As seen in figure 4-2, the overall shape of the curve for methods 1 and 3 are relatively the same as well as methods 2 and 4, both showing there is no positive relation between CI and increased irradiation dose, with a tendency of initial increase after 180 mJ/cm^2 of energy. This result suggests that an accumulation of

carbonyl structures (C double bond O) occurs on the MPs surfaces after low dose irradiation (even under 180 mJ/cm^2) (Lin et al., 2020). The decrease in values could suggest that these C double O bonds were degraded when the irradiation dose increased continuously. All four methods showed similar maximum percentage increases in CI between 55% and 60%, indicating all methods can determine a similar degree of aging relative to the pristine sample. The steep decrease observed in methods 2 and 4 could be attributed to the large width of the peak at 1675 cm^{-1} after 180 mJ of energy. Wide peaks indicate the presence of exchangeable protons, typically from a carboxylic acid group. This shows that the bonds associated with carbonyl groups are beginning to form at the 180 mJ point and that bonds have fully formed at the 1080 mJ point (Clark, 2023).

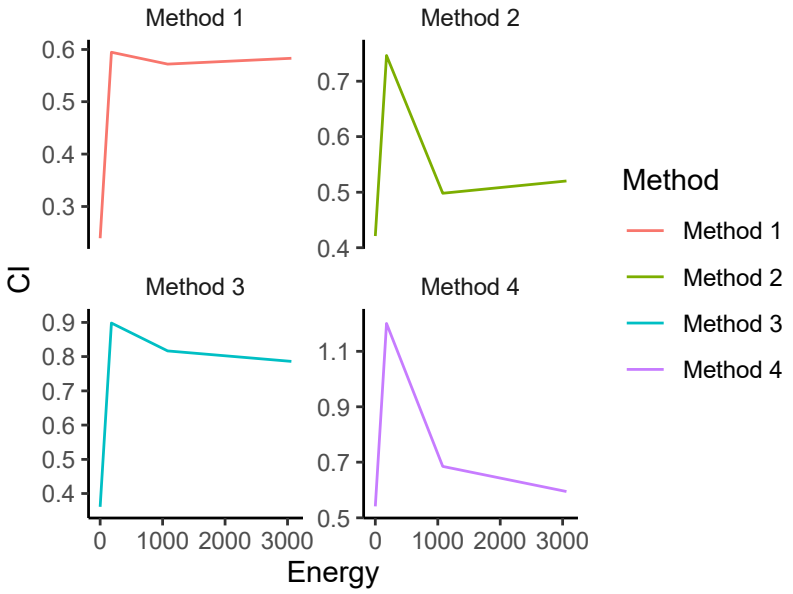

Figure 4-2 *Plots for method comparison of carbonyl indices.*

While both methods 2 and 4 yielded similar results, the method using the area under the curve is less studied and not widely used for measuring carbonyl indices. For comparison purposes,

method 3 was used as it is the most widely used method within the literature (Li et al., 1991; Song et al., 2017; Yousif & Haddad, 2013).

4.2.3 SEM Analysis

After UV aging, alterations in surface morphology can be seen in figure 4-3, including cracks, wrinkles, flaking and overall size reduction of some particles from SEM images below. No significant surface changes were observed through imaging for irradiation doses at 180 mJ/cm^2 (Figure 4-3). As irradiation increased, the surface cracks located on the particles became more pronounced, and flaking of the outer edges of the particles was observed; this degradation is outlined in red in figure 4.3. These changes in cracks and wrinkles may lead to an increase in the overall surface area of the particle, which may, in turn, expose more adsorption sites for contaminants to attach to. Amorphous polymers such as the polystyrene used in this research are particularly susceptible to crack development because of their relatively open structure, which leaves them susceptible to contaminant penetration (Ho et al., 2020). Under conditions commonly encountered in the environment, such crack formation can be accelerated by localized plasticization, which can be described as changes in the mechanical and thermal properties of a polymer lowering its rigidity. Along with an increase in surface area, the flaking aspect also produces nano plastics from microplastics. These particles are extremely small and generally go undetected due to this. These particles could still adsorb many different contaminants that could end up within a distribution system.

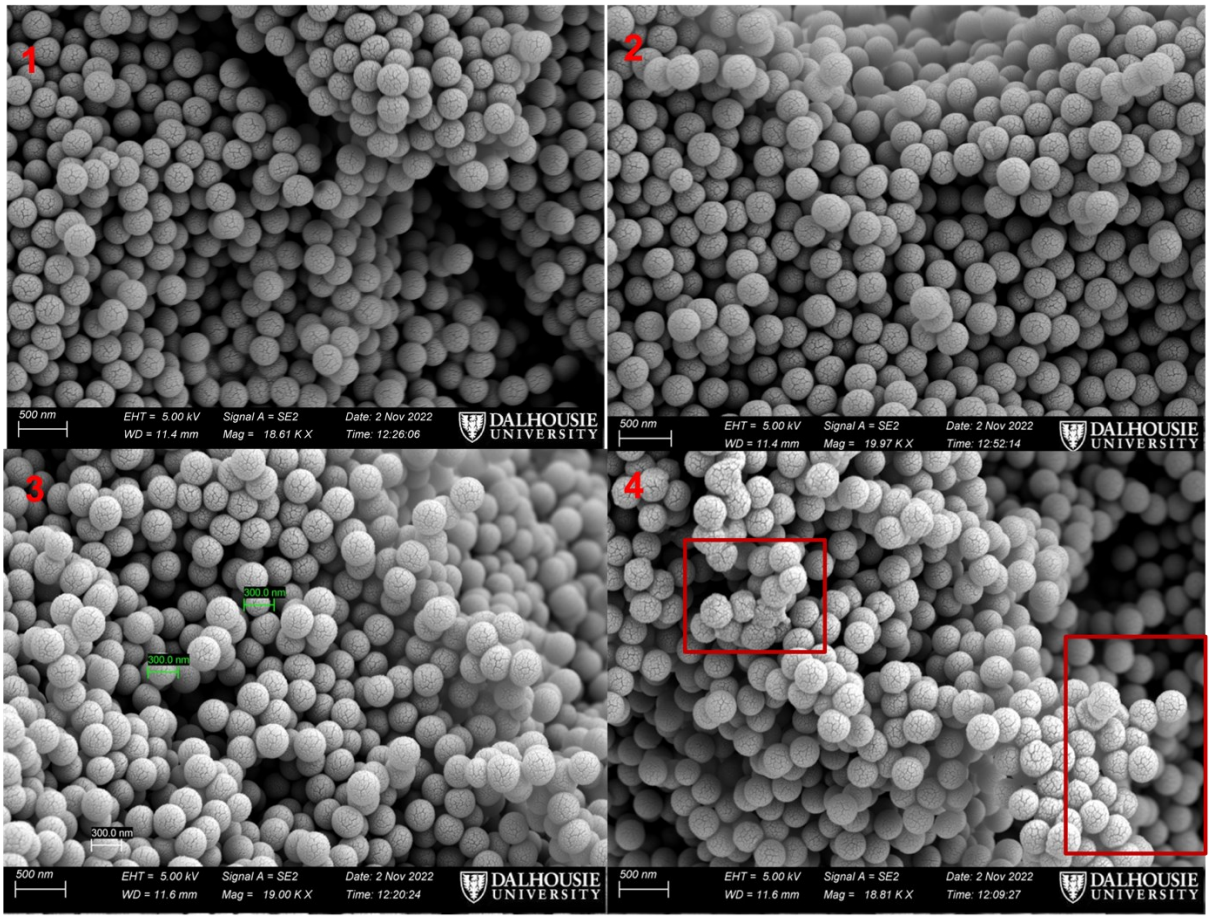

Figure 4-3 *SEM images of irradiated 0.3um polystyrene beads 1. No UV treatment, 2.180 mJ/cm^2, 3. 1080 mJ/cm^2, 4. 3060 mJ/cm^2 between 18 to 20 KX magnification.*

Image J (*ImageJ*, n.d.) was used to better understand and quantify the SEM images seen in Figure 4-3. Figure 4-4 shows the changes in surface measurements compared to the given dosages of UV.

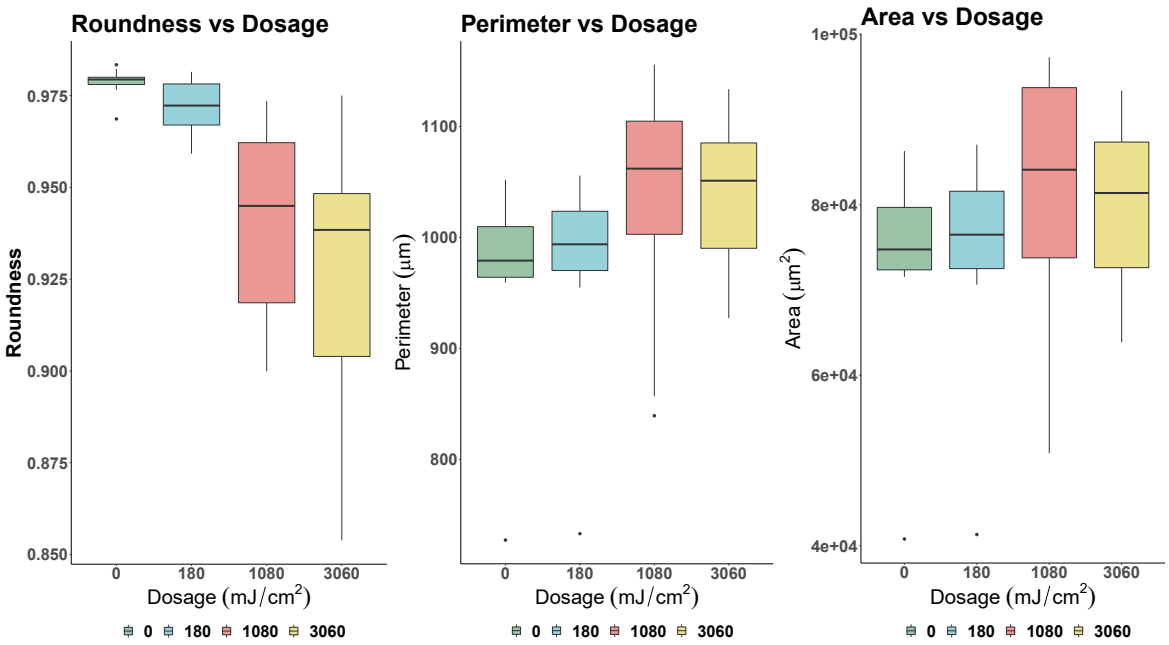

Figure 4-4 *Roundness, perimeter and area changes of microplastics based on UV dosage.*

As seen in the figure above, both perimeter and area have increased with increases in dosage while roundness has decreased. This is due to the increased surface cracks and wrinkles that have formed on the surface of the plastic, which are seen in the SEM imaging. The variability has also increased for all measurements as the dosage increased. This variability allows for samples to be more environmentally relevant since samples found within both water and wastewater treatment plants have a wide variety of shapes/sizes and surface morphologies (Pivokonsky et al., 2018).

4.3 Conclusion

The tests conducted aimed to determine if using a collimated beam would be a sufficient rapid method for in-lab aging of microplastics for testing purposes. It was noted that shifts in the FTIR spectra occurred, showing the formation of carbonyl bands. These carbonyl bands were used to quantify aging using the CI indices, which according to the literature were able to show significant weathering occurred. The SEM imaging further indicated weathering was present due to the changes in area, perimeter, and surface area.

One advantage of using UV irradiation as an aging method is that it can be easily replicated in different laboratory settings. This makes it possible to compare the results of different studies and draw meaningful conclusions about the impact of aging on microplastics. In addition, UV irradiation is a cost-effective and efficient method that does not require the use of hazardous chemicals or specialized equipment. This makes it a practical method for use in research and testing laboratories. Overall, the use of UV irradiation as a method for aging microplastics in the laboratory is a reliable and effective approach that can help to advance our understanding of the environmental impact of microplastics.

Chapter 5 Removal Efficiency of microplastics in both drinking/wastewater using conventional treatment

5.1 Introduction

Even though MPs are a global emerging contaminant, systems for mitigating and controlling them are not well established. There is currently a lack of knowledge on how very small (< 20μm) microplastics can be removed by conventional water treatment processes, specifically a coagulation/flocculation/sedimentation treatment train. Presently, this process has shown poor removal efficiency on pristine particles using in-lab trials (Lapointe et al., 2020). The low removal rate may be attributed to the lack of interaction between coagulants and the pristine plastic surfaces. In the environment, these plastics would be exposed to some level of photodegradation as well as fragmentation, and mechanical abrasion, which would result in changes the porosity and surface chemistry of the particle, which could increase interactions with the coagulant used (Munoz et al., 2021). The particles would also likely be coated with Natural Organic Matter (NOM) and silica-based colloids that are present in the water sample (Wilkinson et al., 1997).

Most studies have shown that the greater the size of the microplastic, the better the removal efficiency will be since larger particles are more likely to attach to floccs than smaller ones, resulting in a higher amount settling in the water (Zhang et al., 2020a). Previous studies have shown that 90% of MPs present in effluent treated by coagulation/flocculation are sized smaller than 20μm. A study conducted by Pivonkonsky et al. (2018) aimed to quantify the number of microplastics larger than 1μm being removed through conventional drinking water treatment, to understand the amount, size and makeup of microplastics being introduced into the drinking

water system (Pivokonsky et al., 2018). This study tested three water treatment processes, all employing coagulation/flocculation with different filtering techniques. It was shown that for all three plants the coagulation process removed between 40% and 55% of total microplastics from the influent (Pivokonsky et al., 2018). These values are much higher than removal achieved by granular activated carbon (GAC) filtration (20%) and deep filtration (6%) alone, which indicates that the coagulation process is the main driver for microplastic removal in a drinking water system.

The primary objective of this study was to identify the removal efficiency of microplastics via coagulation under different matrix conditions (e.g., raw water influent and wastewater influent, aged vs unaged PS). The secondary objective was to determine the accuracy of using spectrophotometry for microplastic detection by using changes in single wavelength absorbance values to determine removal. This study compared various sizes (0.3µm, 1.1µm, 3.0µm) of PS beads to understand the influence size has on the detection method to further guide the study.

Once a detection method was established, the study investigated the removal behaviors of MPs using conventional coagulation/flocculation/sedimentation characterized by initial influent turbidities and alterations to the PS surface. Finally, the study compared the removal behaviours of MPs within wastewater influents, characterized by increasing initial turbidities, using conventional coagulant coupled with a cationic polymer additive. This is of increasing importance due to wastewater effluent being a primary source of microplastics within the environment (Bretas Alvim et al., 2020).

5.2 Results: Detection Method

The correlation between the detected levels of microplastics and UV absorbance was linear for microplastics sized at 0.3 µm. Particles larger than 1 µm show a less linear trend as size increases (Figure 5-1). As particle size increased, the slope became smaller, which can be further seen in the decrease in R – squared values. This is probably caused by a smaller number of particles/L present in the sample for larger particles than for those samples with smaller particles. Samples using 3 µm MPs had an average count of $6.7x10^{8}$ MP/L, while samples using 0.3 µm MPs had $6.7x10^{11}$ MP/L, which is 1000 times greater, meaning there is much more surface area for light to interact with within the sample. Number of particles per L were found using equation 2, which was derived from work done by (Leusch & Ziajahromi, 2021). This theory is supported by a study completed in 2014, which showed that for particles larger than 60 nm, an increase in size corresponds to a decrease in absorbance (Goh et al., 2014).

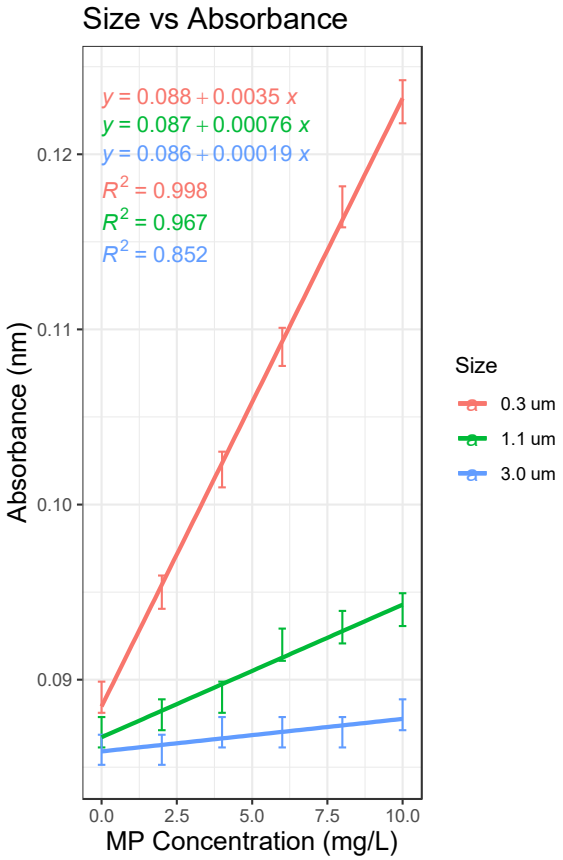

Figure 5-1 *Calibration curve for 0.3,1.1 and 3.0µm polystyrene spheres at an absorbance wavelength of 290 nm.*

$$x\left(\frac{Particles}{L}\right) = \frac{Concentration\ of\ plastics\left(\frac{mg}{L}\right)\times 10^{9}(unit\ conversion\ factor)}{\left(\frac{\pi}{6}\right)\times \text{density of particle}\left(\frac{g}{cm^{3}}\right)\times[diameter\ of\ particle\ (\mu m)]^{3}} \quad \textbf{(5)}$$

The method employing the HACH for spectrophotometry as a simple detection method showed promising results for quantifying the removal efficiency of a known analyte. At a treatment facility, this method could be used to test coagulation efficiency for a known MP and could be used as an indicator for removal efficiency of MPs for different coagulation/flocculation/sedimentation parameters. To account for matrix effects, a calibration curve must be made for each new water sample, ensuring to take a blank reading to account for any material within the influent that may absorb light at the same wavelength as the given MP.

This method would not be feasible for environmental samples since initial concentrations of analytes would be unknown. For MP quantification of environmental samples, a different method would need to be used.

5.2.1 Calibration Curves: Drinking Water

In drinking water treatment, specifically at Pockwock Lake, influents are filtered through a dual media filter (anthracite and sand) with an estimated effective pore size of 1.2 µm, meaning larger plastics would ultimately be removed by just filtration. Any plastic smaller than this threshold is subject to move through the filter, through the treatment plant and out to distribution if it is not removed by another method. To determine if removal (if any) is achieved, a method which can detect microplastics of very small sizes needs to be employed. Therefore, using spectrophotometry at a single wavelength absorbance of 290 nm was used. This method can currently only be employed for one type of plastic material at a time, and a calibration curve must be completed for each new influent. For drinking water, turbidity levels ranged from 2.4 to 0.74 NTU. The r^2 value for all calibration curves was >0.99, meaning that turbidity at these levels have a marginal impact on the fit of the calibration line. The regression line for UV absorbance parameters are shown in Table 5-1.

Table 5-1 *Regression line parameters for coagulated drinking water.*

Trail Number	Experimental Condition	Raw Turbidity (NTU)	Coagulated Turbidity (NTU)	R^2	Slope	Intercept	95% Confidence Interval on slope
1	1	0.741NTU	0.46 NTU	0.9965	4.3×10^{-3}	0.049	0.0039-0.0050
2	1	0.888 NTU	0.493 NTU	0.9988	4.6×10^{-3}	0.043	0.0042-0.0048
3	1	1.56 NTU	0.581 NTU	0.9960	4.5×10^{-3}	0.037	0.0043-0.0048
4	1	2.44 NTU	0.589 NTU	0.9935	4.5×10^{-3}	0.037	0.0039-0.0047

To study the repeatability of the results, three separate spiked calibrations were performed for each matrix. The standard deviation of these replicates is reported as error bars in the calibration curves. The range of the confidence intervals for all four trails have significant overlap, showing that the raw turbidity has little effect on the variation of the slope. The maximum residual standard error for each calibration curve was 0.0026 mg/L for raw water samples and 0.0015 mg/L for coagulated samples. The coagulated water calibration curves are shown in Figure 3 below, with standard deviation being expressed as error bars. The calibration curves for the raw water can be found in Appendix A.

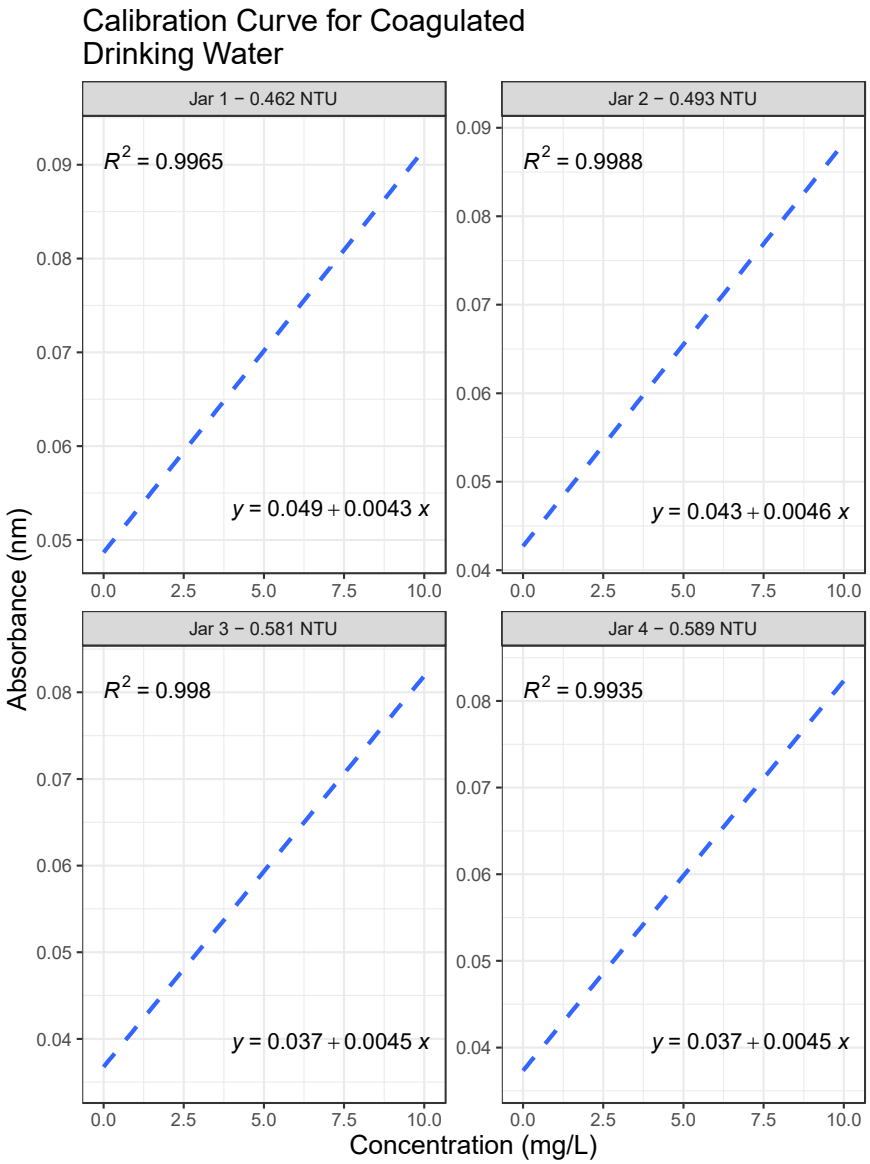

Figure 5-2 *Calibration curve for coagulated water of varying influent turbidity's using experimental condition 1.*

5.2.2 Calibration Curves: Wastewater

For wastewater, the variance in turbidity levels ranged from 60 to 240 NTU. The r^2 value for all treated calibration curves can be seen in the table below. More turbid water samples responded better to treatment, resulting in lower-level effluent turbidities. This is likely due to the increased

particle-to-particle collisions and flocc formations present in more turbid waters variability. The line parameters are shown in Table 5-2.

Table 5-2 *Regression line parameters for coagulated wastewater.*

Trial Number	Experimental Condition	Raw Turbidity (NTU)	Coagulated Turbidity (NTU)	R2	Slope	Intercept	95% Confidence Interval on slope
1	4	60	31	0.9890	5.0×10^{-3}	0.67	0.0043-0.0055
2	4	140	27	0.9930	3.6×10^{-3}	0.2	0.0027-0.0041
3	4	200	21	0.9970	4.5×10^{-3}	0.44	0.0042-0.0049
4	4	260	18	0.9970	4.4×10^{-3}	0.68	0.0041-0.0049

To study the repeatability of the results, three separate spiked calibrations were performed for each matrix. The coagulated water calibration curves are shown in Figure 5-3 below with standard deviation being expressed as error bars. The calibration curves for the raw water can be found in Appendix A. As turbidity increased, the range of the confidence interval decreased, showing that on samples where treatment was more effective (lower coagulated turbidity) the slope was estimated with less uncertainty.

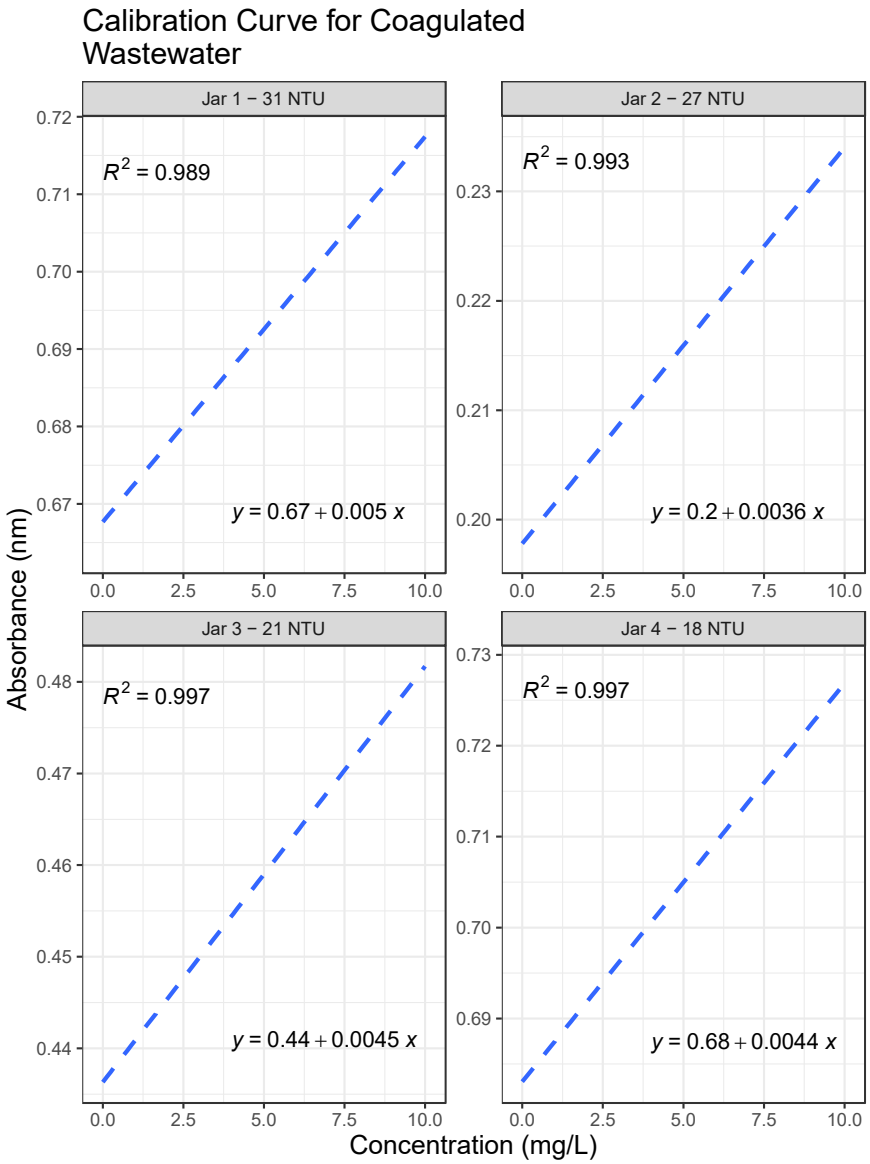

Figure 5-3 *Calibration curves for varying turbidities of coagulated wastewater using experimental condition 4.*

5.3 Results: Removal of microplastics from water treatment

5.3.1: Removal from drinking water systems

The aim of this study was to evaluate the effect that aluminum sulfate as a coagulant would have on microplastic removal, and how increases in turbidity levels could impact removal within a raw water matrix. This study focused on MPs sized at 0.3 µm as they show increased challenges

in removal due to their size. Microplastic removal was detected after coagulation/flocculation/sedimentation treatment. Removal was quantified by looking at changes in single wavelength absorbance values of 290 nm, which is the corresponding wavelength for polystyrene microspheres (Li et al., n.d.). This removal was compared to varying levels of turbidity which are commonly seen in raw water samples (< 5.0 NTU) (Canada, 2005, p. 8) to determine what impact increasing turbidity levels had on removal efficiency of microplastics. Error bars were set using the maximum and minimum values for all triplicate values.

After a 40-minute sedimentation time, little to no MP removal was observed in samples containing no coagulant. This demonstrates that new polystyrene beads, having a similar density to water ($1.05 g/cm^3$), would not be effectively settled out. However, previous studies have shown that biofilm growth on the surface of plastic can occur after 24 hours and cause settling to occur without the addition of coagulant (Huang et al., 2021; Kaiser et al., 2017; Semcesen & Wells, 2021).

The highest MPs removal (86 ± 3%) was achieved in raw water with the highest turbidity (2.44 NTU) corresponding to 8.47 mg/L removed. Samples having a lower turbidity showed removal values of 5.95 mg/L, which corresponds to a removal rate of 59% (± 3%). The relationship between percent removal and initial turbidity levels is illustrated in the Figure 5-4. As turbidity increases, removal efficiency also increases. This suggests that higher levels of organics (higher turbidities) have higher particle concentrations, which increases the opportunity for particle-particle collisions in the system, entrapping the MPs, and increasing aggregation rates (Farrell et al., 2018).

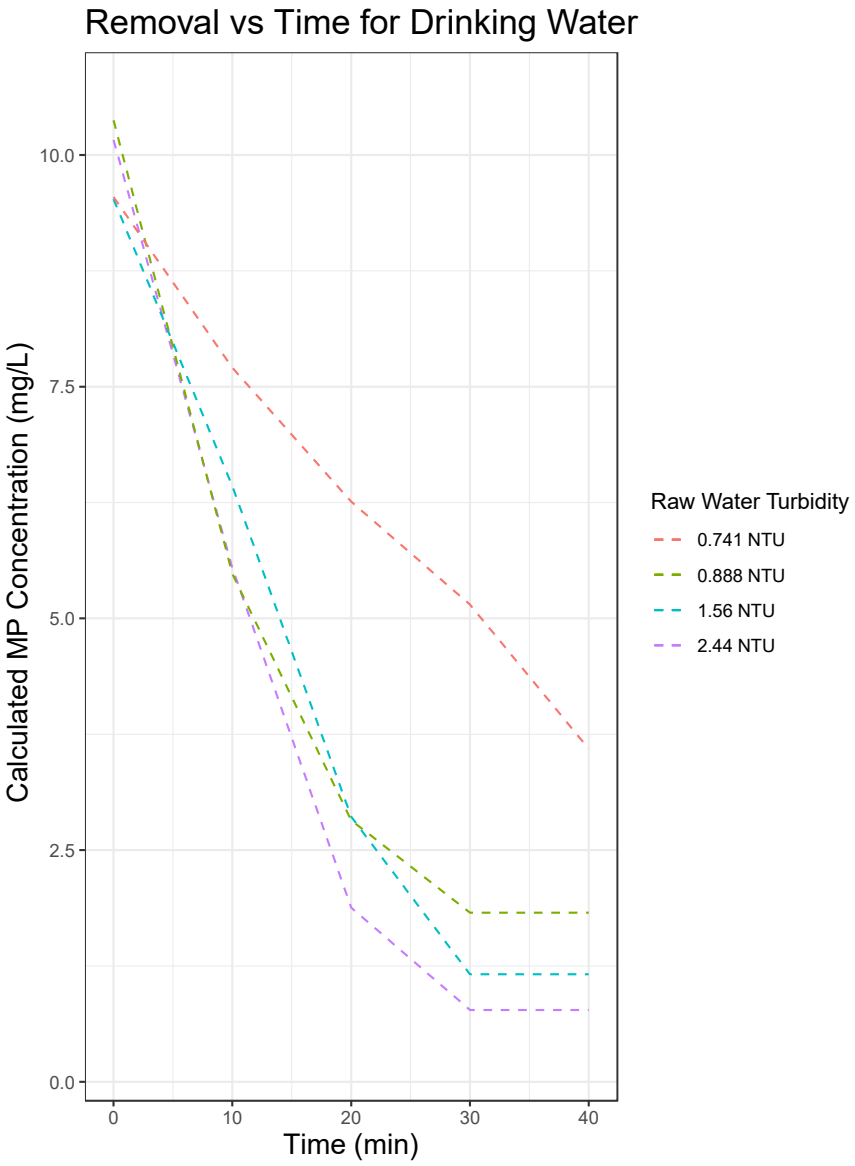

Figure 5-4 *Microplastic concentration vs Settling Time using raw drinking water influent.*

Particles of this size (0.3µm) tend to agglomerate and self-aggregate due to Brownian motion, and small amounts of settling have been observed after 24 hours in the absence of coagulant in similar studies (Ghernaout, 2015). The likely main mechanism causing the removal of microplastics is charge neutralization. The zeta potential of the polystyrene microplastics was measured to be -13.89 mV at a pH of 6.5 in DI water. As the turbidity levels increased, so did the

negative charge of the sample, having a maximum negative zeta potential of -26.64 mV. When compared to samples containing no PS, the negative charge was significantly lower than those with PS present, meaning the combination of NOM and PS was a main factor for the highly negative samples. Based on coagulation theory, the negatively charged microplastics are likely to interact with positively charged aluminum hydroxide. As mixing occurs, the particles may become enmeshed by sweep flocculation in a mass of amorphous aluminum hydroxide (Sun et al., 2019). Once treatment was completed, the average zeta potential for samples containing PS had an average increase of 57% having maximum zeta potential of -12.46 mV. This shows that the main mechanism responsible for MP removal within these water matrices was probably charge neutralization.

Though up to 86% removal was achieved following CFS treatment, there are still significant concentrations of microplastics remaining in the effluent. Pockwock filtration pore sizes are 40 µm, with an estimated effective pore size of 1.2 µm after filter ripening. At these sizes, the system would not be able to capture these microplastics. A study conducted in 2022 found that although between 70-85% of all microplastics present in raw water can be removed with a CFS, of the plastics remaining in the treated effluent , 92% were < 10µm (Mason et al., 2016; Pivokonsky et al., 2018). These plastics were found in concentrations of 628 ± 28 MPs/L. This concentration is much lower than that used in this study, but significant negative impacts are still prevalent at these concentrations. The knowledge gap on microplastics does not give an indication of what levels should begin to raise concern for human health but it is known that microplastics are ubiquitous in almost all environmental matrices.

5.3.2 Removal of aged microplastics using CSF

The aim of this study was to determine what impact in lab weathering had on MP removal during conventional treatment. This study focused on MPs sized at 0.3µm, as particles of this size and smaller show significant difficulty in removal. Removal was quantified by looking at changes in single wavelength absorbance values of 290nm, which is the corresponding wavelength for polystyrene microspheres. This removal was compared to varying levels of weathering, which were used to simulate different environmental samples. Error bars were set using the maximum and minimum values for all triplicate values. The initial turbidity of the raw water sample was 1.8 NTU.

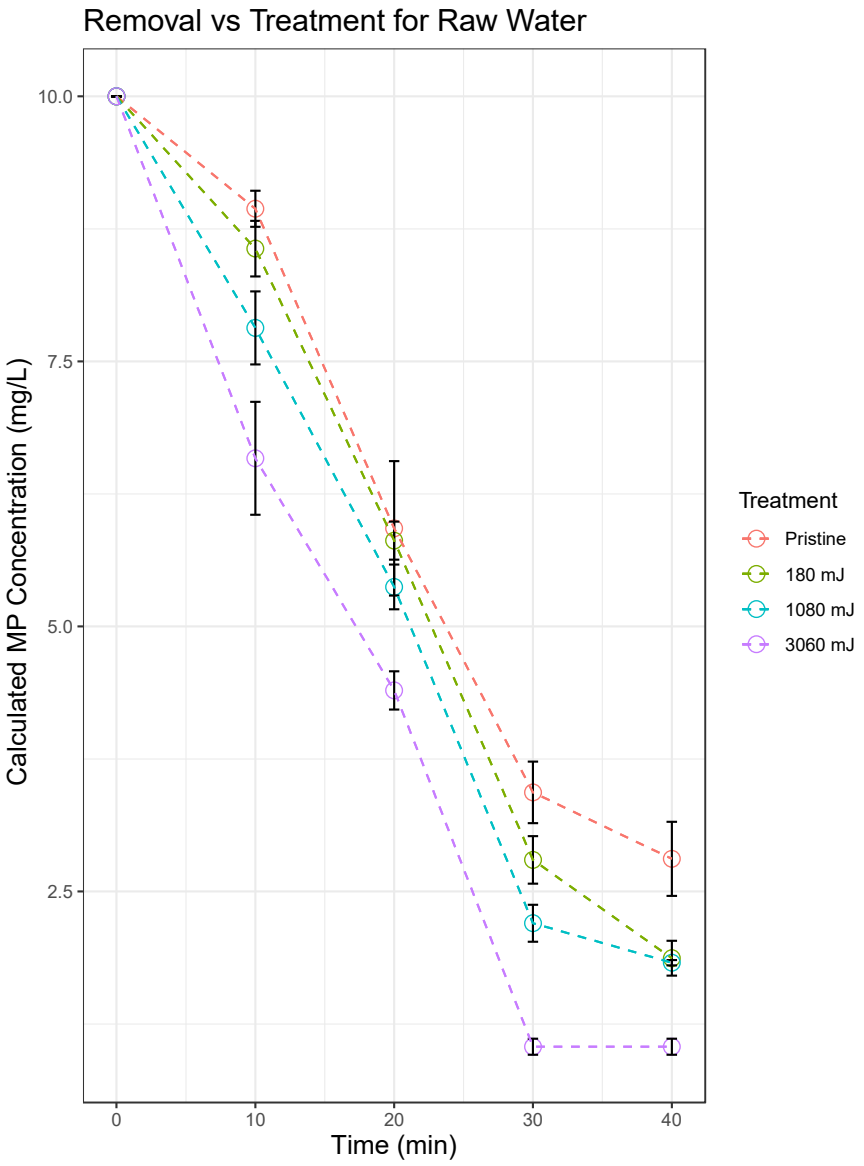

Figure 5-5 *Jar testing using plastics of varying degrees of weathering using 0.3um polystyrene microplastics with samples being spiked at 10 mg/L.*

The highest removal was observed at samples which had been irradiated at 3060 mJ/cm^{2,} which corresponded to a 90% (±1% S.D). The degree of aging and amount of removal were proportional, showing that as weathering became more severe, removal was higher. This could be due to the increased number of functional groups which become present on the surface after irradiation, which is discussed in section 4.2.1.

It should be noted that triplicate jar tests were also conducted using coagulant and microplastics in the absence of organics. The pH was adjusted to 6 with the addition of lime and a buffer was added to maintain alkalinity. No coagulation or flocculation occurred throughout the jar test and no settling was observed, showing that plastics must be in the presence of organics to coagulate for efficient removal. A graph of this can be found in Appendix A.

5.3.3 Removal of microplastics in wastewater

The aim of this study was to evaluate the effect that aluminum sulfate coupled with the addition of polymer would have on microplastic removal, and how increases in turbidity levels could impact removal within a wastewater matrix. This study was conducted on municipal wastewater from a combined sewer system. This means that the influent turbidity levels are highly variable and subject to change due to stormwater dilution. To date, removal of microplastics of this size have not been previously studied in a municipal wastewater matrix. There is a lack of analytical methodology for studying microplastics in wastewater at this size, since generally anything smaller than 10µm in a wastewater matrix is excluded due to high price points and limited access of the highly specialized analytical tools able to detect colloids of these sizes (Mintenig et al., 2017).

After a 40-minute sedimentation time, the data showed that for blank samples containing no coagulant, little to no MP removal was observed, and the absorbance levels stayed consistent. A plot of this data can be found in Appendix A. This means that settling alone could not separate MPs within these water samples at this time frame, which would be attributed to polystyrene beads having a very similar density to water. The highest removal was achieved in waters having

high turbidity levels (260 NTU) at 9.48 mg/L. This corresponds to a removal rate of 96% (± 3% S.D) with samples using both aluminum sulfate coupled with polymer. Error was calculated using standard deviation of replicates (n = 4). Samples having a lower turbidity (60 NTU) showed removal values of 6.89 mg/L, which corresponds to a removal rate of 68% (± 3%). The relationship between percent removal and initial turbidity levels is indicated in the Figure 5.32. As turbidity increases, removal efficiency also increases. Error bars were computed using maximum and minimum value ranges for each replicate.

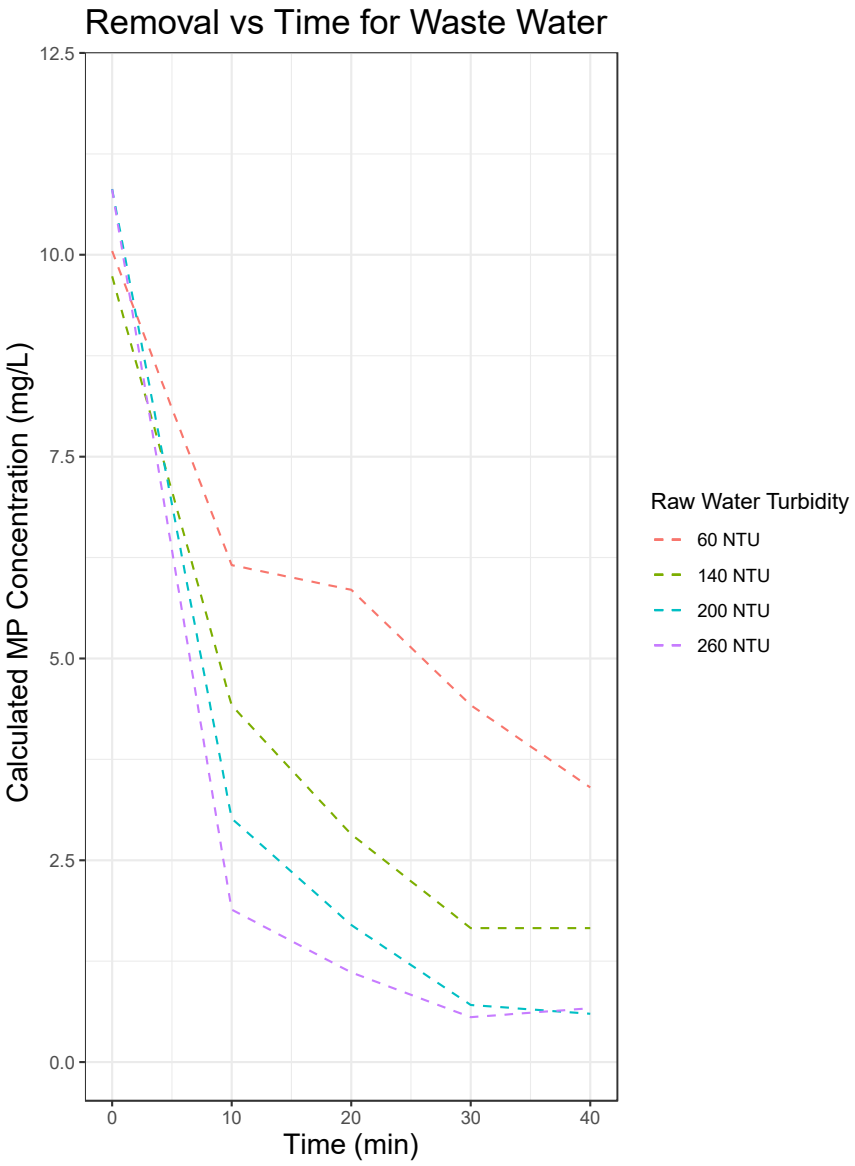

Figure 5-6 *Microplastic Concentration vs Settling time for municipal wastewater with the addition of polymer and coagulant using 0.3um polystyrene microplastics with samples being spiked at 10 mg/L.*

The addition of polymer to the jar tests yielded higher removal of microplastics than the jar tests that did not. The jars containing polymer and coagulant were able to remove an additional 1.5 mg/L of microplastics compared to the jars that did not. This yielded a 5% (±1% S.D) increase in removal when both polymer and coagulant were used. This was calculated by comparing the removal of the microplastics from jars containing polymer and alum vs jars that only contained

alum, and error was computed using the standard deviation of the replicates. This is illustrated in Figure 5-7 using highly turbid water (260 NTU), and all other samples followed these same trends which can be seen in Appendix A.

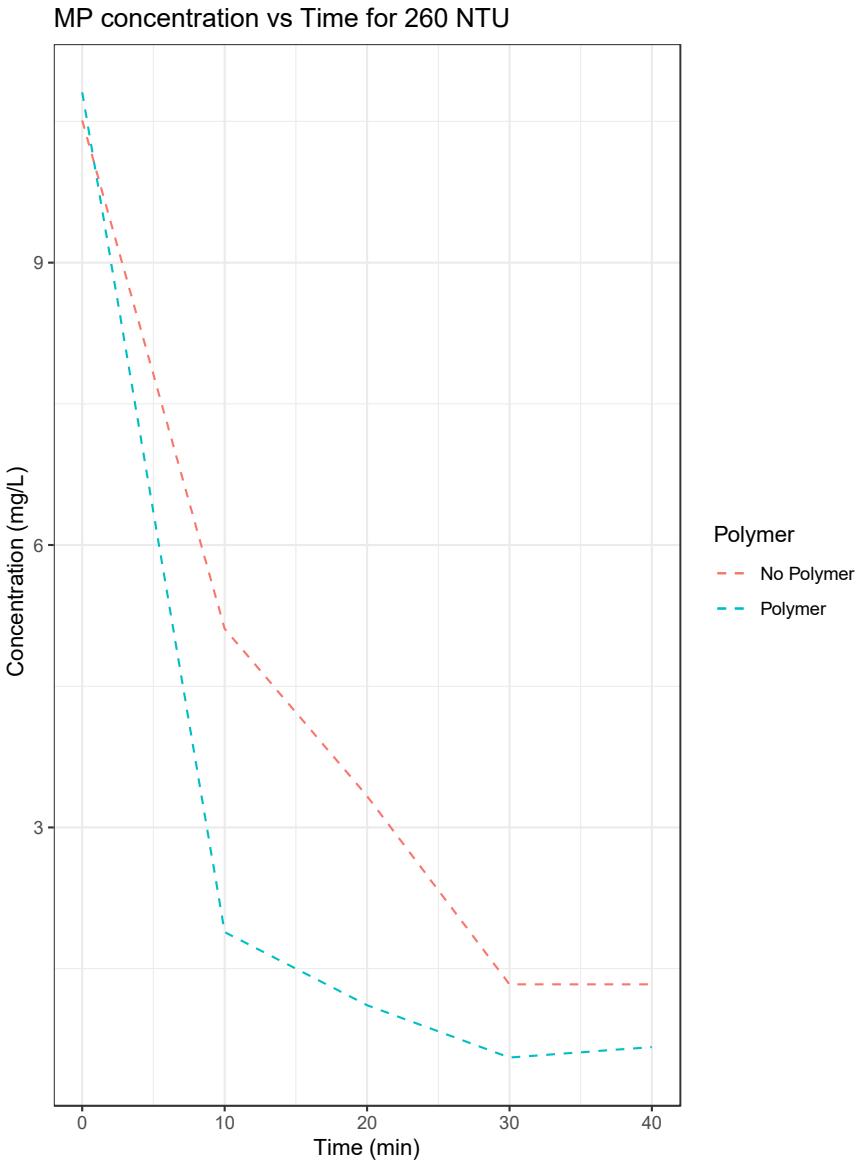

Figure 5-7 *Removal Efficiency of microplastics from 260 NTU wastewater with and without polymer.*

This increase in removal could be caused by the polymer adsorbing onto the surface of the microplastic causing further agglomeration. The interactions between microplastics and chemical flocculants have not been well studied, and how much it aids in removal is unclear. It is known that polymer addition to wastewater aids in flocc formation due to the cationic charge of the polymer, which further aids in the charge neutralization mechanism present in the flocculation (Industries, 2021).

5.3.4 Three-point calibration vs Six-point calibration

The current study utilized a six-point calibration curve for each different water sample. For time and ease of execution, a three-point calibration was tested and compared to the six points to determine if similarly accurate results could be created and if the slopes created would be the same. These calculation errors were summarized and had a maximum slope deviation of approximately 1% for both drinking water and wastewater, meaning that a three-point calibration method could also be used. Figure 5-8 shows calibrations for both drinking water and wastewater samples using both a three-point and a six-point calibration. As turbidity increased, the percent error of the calibration curves did as well.

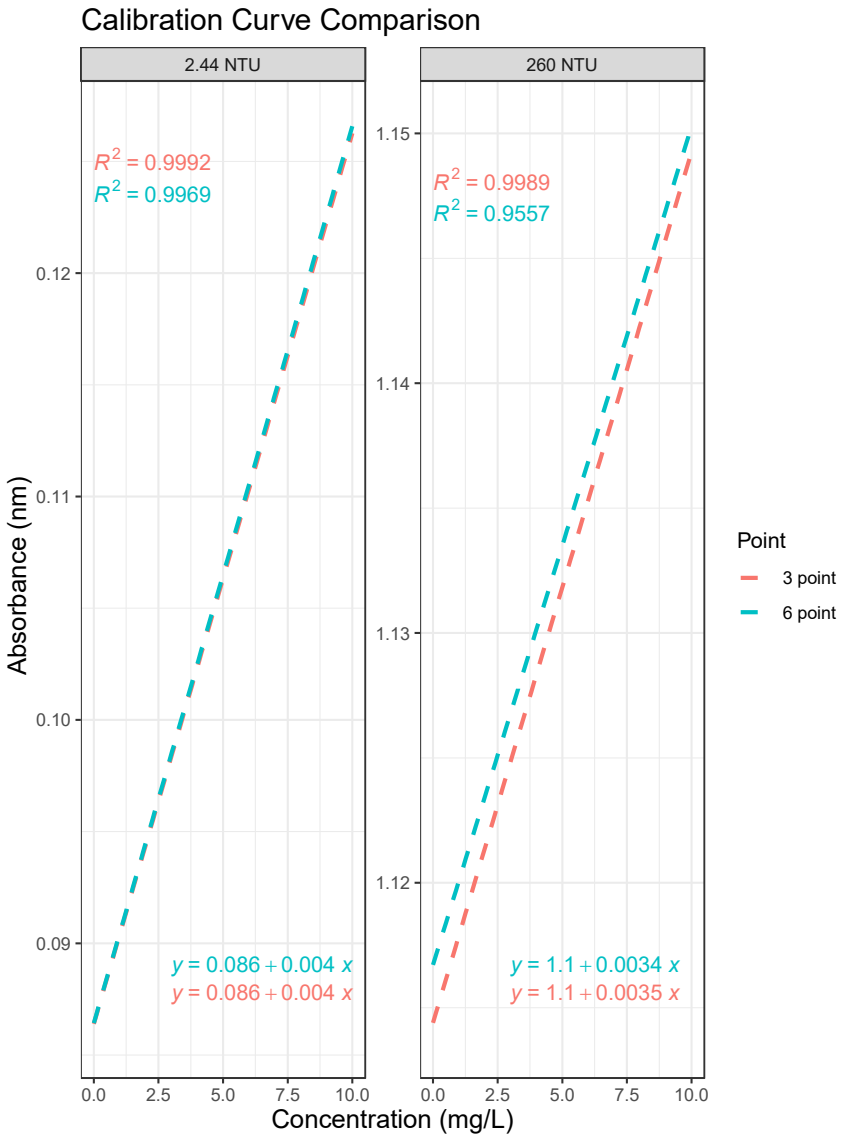

Figure 5-8 *3-point vs 6-point calibration curves for polystyrene detection.*

5.4 Conclusions

The method using spectrophotometry at a single wavelength absorbance showed promising results for detection within drinking water treatment, with an average r^2 of 0.99, regardless of initial turbidity levels. As turbidity levels of raw wastewater increased, the method used became increasingly accurate, due to the increase in flocc formation and treatment performance. The

coagulated turbidity of these samples was lower than those with an initially lower turbidity, meaning that the lower the turbidity of the final matrix, the more accurate the method will be, likely due to less interference of other colloidal material present in the influent.

The removal efficiency of microplastics within a water treatment system is affected by multiple factors, most notably increases in turbidity levels of the influent. The removal efficiency of both drinking water and wastewater followed the same trend, showing greater removal with higher turbidities due to increased particle-particle collisions causing floc formation. For aged plastics, as the degree of surface weathering increased, so did removal. This increase is likely caused by the increased interactions with the coagulant from functional groups present and the increased surface area of aged plastics.

Chapter 6 Aged and non-aged microplastics as a potential vector for heavy metal transport

6.1 Introduction

There is potential for MPs in bodies of water to absorb and transport harmful chemicals or heavy metals (Mendez et al., 2019). This poses challenges for water treatment utilities as the adsorption capability of microplastics is inversely related to their size (Wagner et al., 2014). It is important to understand the amount of heavy metal adsorption relative to a plastic particle size that can occur to determine if maximum allowable concentrations of these toxins in treated water are being exceeded, as well as if different water characteristics can influence adsorption behaviours. Similarly, plastic particles can also be a transport vehicle for natural organic matter (NOM) in differing environments, and NOM could potentially alter the adsorption capacity and toxicity of microplastics. NOM is present in almost all aquatic ecosystems, and concentrations can range from almost zero to more than 20 mg/L (Andersen & Gjessing, 2002).

The adsorption of heavy metals by MPs is likely to change their surface properties and toxic effect. Once these MPs are released into the environment, their mobility, persistence and toxicity in an aquatic system largely depend on their stability and possibility of forming aggregates (Troester et al., 2016). Aggregation is an important process since aggregates containing MPs can likely be removed via a filtration process, while dispersed MPs will be able to diffuse, be more mobile, and have a larger available surface area for adsorption.

MP stability in aquatic systems is governed by their physicochemical properties such as size, coating surface charge, as well as aquatic chemical conditions. These conditions include pH,

ionic composition, and presence of NOM (Cargnello et al., 2014). After an MP enters the environment, it is likely the MP will interact with some form of organic matter, as both ubiquitously exist in aquatic ecosystems. When NOM is exposed to these MPs, it imparts a negative charge and modifies the surface properties by raising their absolute surface potential. This is done through different interactions dependent on the nature of both the organic as well as the MPs. These interactions are mainly dependent on the functional groups present on both species, particularly the aromatic structures on PS are found to interact with the aromatic structures of the dissolved organics through $\pi - \pi$ bonds, and these colloids are then entrapped within the organics, creating an electron-dense co – polymer (Chen et al., 2018; Zhao et al., 2010). This exposure could impact aggregation and adsorption potential based on initial surface charge of the particle.

Furthermore, a weathered microplastic which has undergone physical and chemical changes due to environmental exposure can lead to differences in its surface properties and adsorption capacity. These changes can include the formation of cracks, crevices, and pores on the surface, as well as the creation of functional groups that can interact with heavy metal ions. Therefore, a weathered microplastic may have a higher adsorption capacity for heavy metals than a pristine microplastic due to these modifications, but the extent of the differences will depend on the specific weathering conditions.

The aim of the study is to determine the adsorption capacity of heavy metals to MPs using Pb^{2+} with the presence of NOM and without. This study is aimed to investigate the following objectives:

(1) estimated adsorption of lead onto polystyrene,

(2) the impact of NOM on Pb^{2+} adsorption to polystyrene,

(3) the impact of UV irradiated surface weathering on adsorption capacity

6.1.2 Approach

This study has been set up as a two by three factorial design. The parameters being changed are:

- Plastic Age (2 levels: new and aged)
- Water matrix (Synthetic water, synthetic water + 1 mg/L humic isolate, raw water)

Table 6-1 *Factorial Design set up for batch adsorption experiment.*

Sample ID	Plastic	Water Matrix
1	Aged	Synthetic Water
2	New	Synthetic Water
3	Aged	Synthetic Water + 1 mg/L humic isolate
4	New	Synthetic Water + 1 mg/L humic isolate
5	Aged	Raw Water
6	New	Raw Water

6.2 Results

In jars one and two, the synthetic water contained no added organics, to isolate lead adsorption to MPs to better understand the effect dissolved organic matter has on heavy metal adsorption, as well as to determine how aging of the microplastics affected its adsorbing capacity. Jar one contained microplastics that had been weathered by exposing them to prolonged doses of UV irradiation and jar two contained pristine microplastics, and a control jar was used that contained

no microplastics. The adsorption of Pb on microplastics was broken down by Shen et al. (2021) into three distinctive steps: (i) exterior mass transfer from the liquid to the outer surface of PS MPs; (ii) internal diffusion of the Pb to the adsorption sites, i.e., film-pore diffusion; and (iii) surface adsorption.

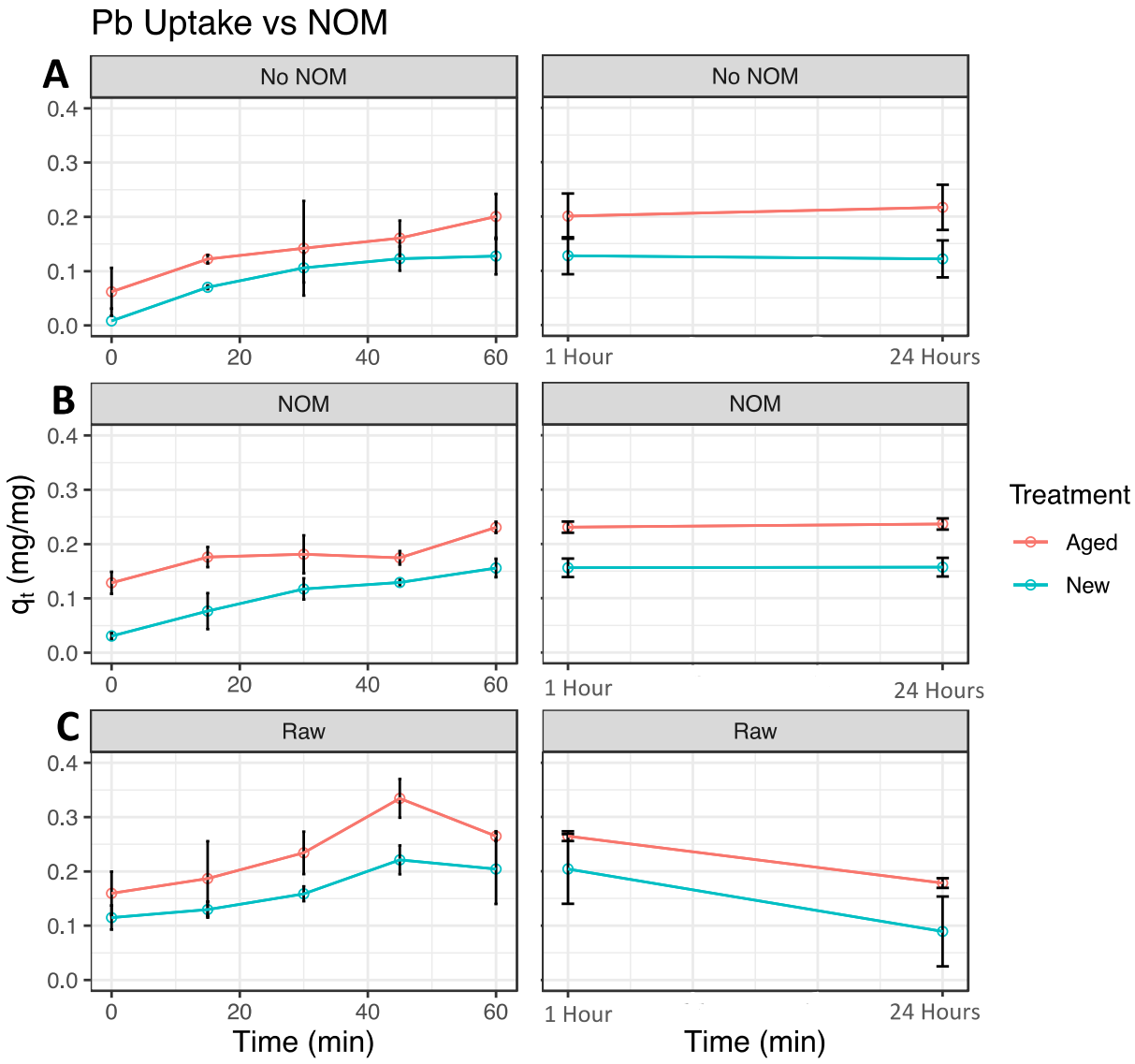

Figure 6-1 *A. Pb uptake vs Time for samples containing no organics B. Pb uptake vs Time for samples containing 1mg/L of humic acid C. Pb uptake vs time for raw water samples for the first hour as well as after 24 hours.*

When no dissolved organic matter was present in solution, the MPs which had been aged showed a higher uptake of lead than those that did not with maximum uptake values of 0.21 mg/mg (± 0.041 mg/mg) and 0.127 mg/mg (± 0.034 mg/mg) , respectively. Error was calculated by using

the range of values from duplicate trials of the experiment. Both samples reached equilibrium within 24-hours of exposure, illustrated by Figure 6-1. A.

For samples three and four, jar three contained weathered microplastics, jar four contained pristine microplastics and a jar with no microplastics were used as a control. This synthetic water sample was identical to that of jars one and two, with the addition of 1 mg/L of HA to mimic DOM. The addition of this showed an increase in metals uptake for both aged and new MPs, having a maximum uptake of 0.23 mg/mg (± 0.041 mg/mg) for aged plastics and 0.157 mg/mg (± 0.017 mg/mg) for new plastics. Both samples reached equilibrium within 24 hours of exposure, illustrated by Figure 6-1. B. These uptake values were 8% higher than the samples containing no organics for aged samples, and 20% higher for pristine samples, which can be seen in Figure 6-2.

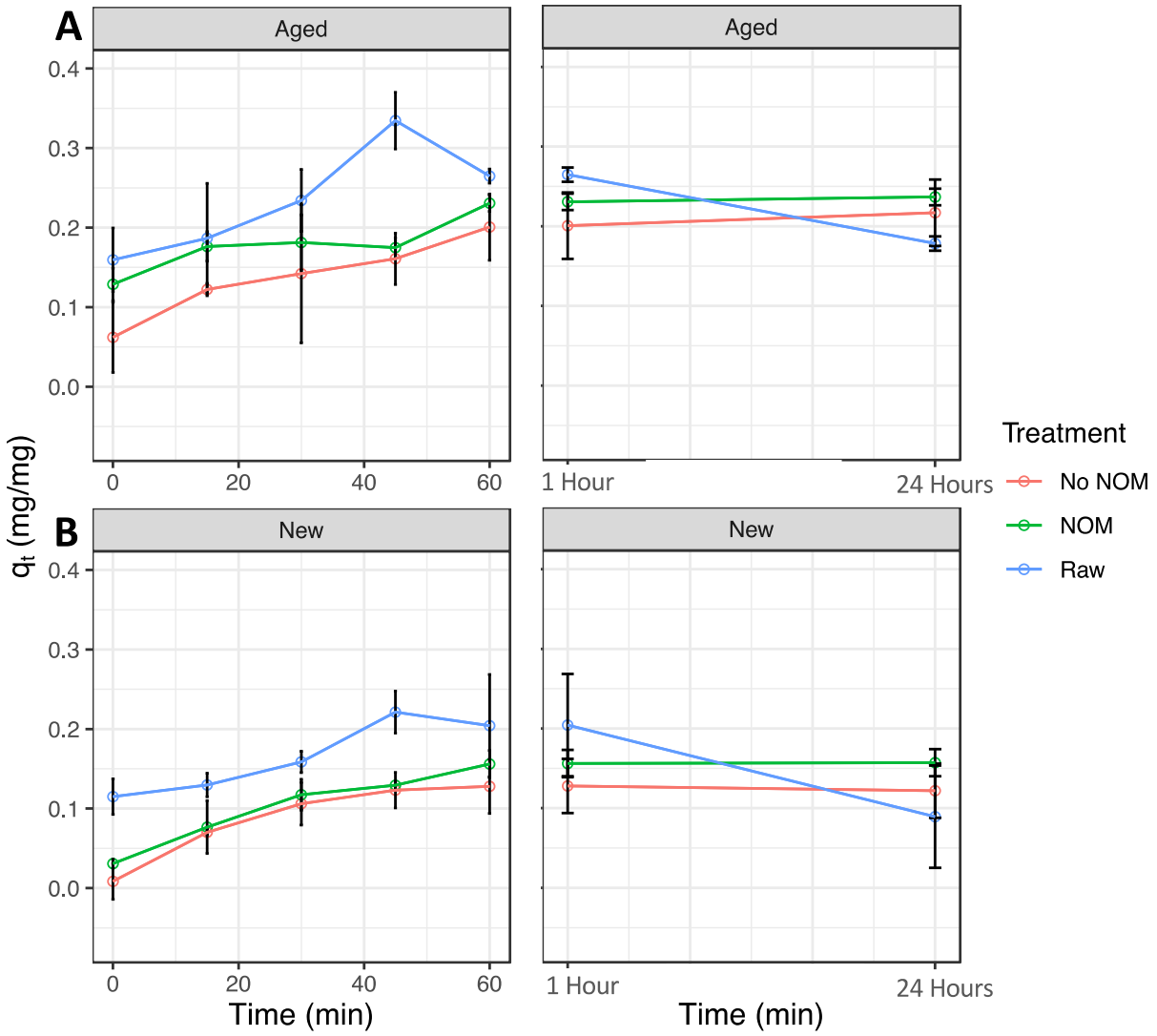

Figure 6-2 *Comparison of Pb uptake dependent on plastic age for the first 60 minutes as well as after 24 hours.*

For samples five and six, raw water from a local watershed was used. Jar 5 contained microplastics that had been artificially weathered through prolonged exposure to UV irradiation and sample 6 contained pristine microplastics. An additional jar was used containing no microplastics as a control. Both TOC and DOC were measured to be 3.8 (± 0.3 S.E) mg/L where n = 4, meaning all the organics within the sample were dissolved in solution. These samples both had maximum adsorption at the 45-minute mark, and a steady linear decrease of desorption after

that, meaning maximum observed adsorption capacity occurred between 45 and 60 minutes of exposure. The aged plastics had a maximum lead uptake of 0.335 mg/mg (± 0.035 mg/mg) while the new had a maximum of 0.221 mg/mg (± 0.027 mg/mg). It should be noted the initial lead values for these samples had the highest initial uptake values compared to the previous two. This means a significant amount of lead was immediately adhering to the MPs during the first minute. Figure 6.2.2 compares the aged vs new plastics when exposed to a known DOM source and an environmental sample. The raw water samples saw the highest overall uptake of Pb, which were 11% higher than those of samples which were spiked with humic acid and 42% higher than samples which contained no organic materials.

The organic content within the environmental sample was not tested for specific types of organics, but it is assumed that a variety of organic species were present within the sample. The level of organics present in the environmental samples were almost four times higher than that of the synthetic waters. Different types of organic species show different interactions with metal ions, due to the different fundamental structures present.

6.3 Discussion

For samples 1 and 2, containing no organics, an increase was seen in the uptake of lead onto microplastics that had been artificially weathered using UV irradiation. This increase in uptake could be attributed to increased surface area or the increased number of functional groups present on the PS surface. These functional groups provide further binding ability for the ionic lead due to their negative charge on the oxygen which has available binding sites (Carlier et al., 1986).

Further information on the increase in surface area and functional group spectrums can be found in section 4.2.1.

The influence of organic matter plays an important role when it comes to heavy metal adsorption. Both samples containing organic content saw a significant increase in Pb uptake compared to samples that contained no organics. HA has a highly negative charge at a pH of 6, a zeta potential around -36 (± 3) mV, which can easily interact with positively charged Pb ions through electrostatic interactions (Coles & Yong, 2006). Previous studies have shown that lead ions interact with HA through cation exchange and hydrogen bonding which have adhered to the surface of the MPs. Lead is bound to the HA on the carboxylic and phenolic functional groups, which both have a high O count, where carboxylate groups are the most abundant. The cationic lead interacts with the negatively charged oxygen within these functional groups (Manceau et al., 1996). The enhanced uptake of Pb ions to the surface of the MPs in the presence of HA may be due to the HA complexes forming a bridge between the Pb species and the MP surface (Chen et al., 2018; Liu et al., 2021). A recent study utilized FTIR spectroscopy coupled with two-dimensional correlation spectroscopy (2DCOS) to investigate the interactions occurring between the MPs and HA. Several peaks were identified as being responsible for NOM – MP interactions due to the change in direction of functional groups and no cross peaks appearing in the 2DCOS maps. These results indicated that the MPs were entrapped by the functional groups within the HA, which formed an electron dense co-polymer (Chen et al., 2018). The Pb cations showed to have a higher affinity for the aged MPs due to the increase of ester functional groups and specific surface areas of these aged plastics. A schematic of these interactions can be seen in Figure 6-3.

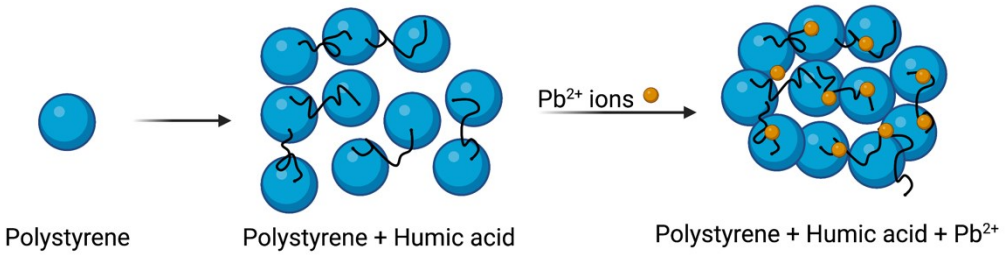

Figure 6-3 *Mechanism of interactions between heavy metals, microplastics and dissolved organics(Wang et al., 2019)*

A recent study found that since PS is a synthesized aromatic hydrocarbon, which behaves similar to benzene, these hydrocarbons contain large portions of condensed domains which increase the nonlinear sorption for HA (Zhang et al., 2018) which could be a reason for the enhanced immediate uptake seen in the environmental samples. This would allow the HA to adhere to the PS surface, as well as the cationic Pb, creating an entrapment of the HA – Pb - MP. This is the likely cause for the environmental sample showing the highest lead uptake, due to the increased amount of organic material present within the sample, since the DOM and polymer have created a co-polymer through cation exchange, hydrogen bonding and π – π bonds (Chen et al., 2018). These co-polymers now have an increased number of electrons which would increase its total electrostatic attraction to the lead cations. Furthermore, the increased ester functional groups that are found on the aged plastics and the increased surface area would also aid in the adsorption of hydrophilic organic structures (Faghihnejad & Zheng, 2013).

It was assumed that after 45 minutes of exposure desorption occurred in the raw water samples since the concentration of Pb in the aqueous phase began to increase. This desorption may be due to the type of adsorption mechanisms responsible for the initial uptake. The HA and subsequent Pb ions to the MPs are likely held by π – π bonds, hydrogen bonds and electrostatic attraction.

These are all bonds that are relatively weak and reversible; along with the samples being kept moving for 24 hours, this movement and constant agitation of the sample may have broken these weak bonds that had formed (Atugoda et al., 2021).

6.4 Conclusions

The batch adsorption experiments conducted aimed to determine the adsorption capacity of lead onto polystyrene MPs under a variety of circumstances. Aged microplastics had a greater adsorption capacity than those that were pristine by approximately 40%, likely due to the increased surface area and altered functional groups present on the surface. In the presence of organic matter, the organics can act as a bridging mechanism between the surface of the plastic and the Pb which increased the overall uptake of Pb. As the organic levels increased, so did the uptake of metals.

Chapter 7 Conclusions and Recommendations

7.1 Conclusions

The purpose of this study was to evaluate the use and effectiveness of a collimated beam for a rapid in-lab aging technique for microplastics. Furthermore, how weathered polystyrene beads behaved compared to pristine during conventional treatment as well as during adsorption kinetic tests. Experiments consisted of three phases with the first being the development of an in-lab method for aging microplastics.

The key findings from the first phase showed this method was able to contribute to significant surface weathering and aging of the PS at increased doses of energy. The changes in surface morphology were shown with SEM imaging and quantified using Image J.
FTIR spectra was also used to show changes in functional groups on the surface of the PS, as well as to compare to known environmental PS FTIR spectra samples. These spectra changes matched those of PS that was taken from environmental samples. These changes were used to quantify aging degree using the carbonyl index. The plastics saw a degree of weathering of approximately 60%. With this evidence, this in-lab method for aging is an appropriate method to mimic environmental plastics for in-lab experimental use.

The second phase of these objectives were to test these weathered plastics to determine their removal efficiency under conventional treatment employed at local water utilities. This study was conducted during the summer months of 2022. The turbidity levels of raw water ranged from 0.74 – 2.44 NTU and wastewater influent levels were between 60 – 260 NTU. It was observed that as the turbidity levels increased, so did removal efficiency, likely due to the

increased number of particle-to-particle interactions occurring during flocc formation. The aged microplastics were also tested using conventional treatment at a turbidity level of 1.8 NTU, and it was observed that the higher the degree of aging of the microplastic, the increased amount of removal was proportional. This was likely due to the increased amount of surface area and functional groups present on the surface which interacts with the both the coagulant and NOM present.

The last phase of the experimental work was to determine if these aged microplastics showed a higher affinity for heavy metals in differing solutions than those that were new. The aged plastics showed an increased uptake of metals by 8% compared to the new plastics, within synthetic water samples where no organics were present. This is due to the increased surface area and increased functional groups present on the surface. In the presence of DOM, the increased number of organics increased the amount of metal uptake to the plastics. This is likely due to the organics within the solution causing a bridging effect between the plastics surface and the heavy metals.

These findings provide important insights into the behaviour of microplastics in water treatment systems, as well as the potential for microplastics to adsorb and transport harmful pollutants such as lead. This knowledge can be used to develop more effective water treatment strategies that account for the behaviour of microplastics, as well as to inform policies aimed at reducing the release of microplastics into the environment. Further research can build upon these findings to explore the mechanisms underlying microplastic aging and adsorption and to investigate the potential impacts of microplastics and associated pollutants on human and environmental health.

7.2 Recommendations

Future studies should be conducted using influents at different times in the year, to determine if/how seasonality would impact the removal of PS using conventional treatment. This would also allow for multiple repetitions of the study to be conducted for a more accurate picture of how much removal is occurring. These studies could also evaluate the effect of different treatment variables, such as pH, temperature, and flow rate, on the efficiency of microplastic removal during conventional treatment. This will help to identify the optimal conditions for microplastic removal and may lead to the development of more effective treatment strategies.

Long-term monitoring of microplastic removal during conventional treatment is necessary to assess the long-term effectiveness of treatment strategies and to identify any changes or trends in microplastic removal efficiency over time.

Overall, quantifying the amount of microplastics removed during conventional treatment is an important step towards mitigating the environmental impact of microplastics. Future work in this area should focus on improving the accuracy and reliability of methods used for detection and quantification, and on optimizing treatment strategies to enhance microplastic removal efficiency.

For future work regarding metals adsorption to PS, studies should employ further analytical measurements such as FTIR spectra comparison, XPS and contact angle. These would allow for a better understanding of what adsorption mechanisms are responsible for the metal's uptake to the aged and unaged plastics. These studies could also assess the effect of environmental factors

such as natural organic matter, dissolved ions, and temperature on the adsorption of lead to polystyrene. These factors can affect the properties of the polystyrene surface and can have an impact on the adsorption capacity of polystyrene.

Overall, quantifying the amount of lead adsorption to polystyrene is an important step towards developing effective remediation strategies for lead-contaminated environments. Future work in this area should focus on improving the accuracy and reliability of methods used for detection and quantification, and on optimizing experimental conditions to enhance lead adsorption efficiency.

References

Abedi, M., Ahangari Cohan, R., Shafiee Ardestani, M., & Davami, F. (2019). Comparison of polystyrene versus cycloolefin microplates in absorbance measurements in the UV/VIS region of the spectrum. *Journal of Shahrekord University of Medical Sciences*, *21*, 110–113. https://doi.org/10.34172/jsums.2019.19

Almond, J., Sugumaar, P., Wenzel, M. N., Hill, G., & Wallis, C. (2020). Determination of the carbonyl index of polyethylene and polypropylene using specified area under band methodology with ATR-FTIR spectroscopy. *E-Polymers*, *20*(1), 369–381. https://doi.org/10.1515/epoly-2020-0041

Andersen, D., & Gjessing, E. (2002). Natural organic matter (NOM) in a limed lake and its tributaries. *Water Research*, *36*, 2372–2382. https://doi.org/10.1016/S0043-1354(01)00432-8

Arangdad, K., Yildirim, E., Detwiler, A., Cleven, C. D., Burk, C., Shamey, R., Pasquinelli, M. A., Freeman, H. S., & El-Shafei, A. (2019). Influence of UV stabilizers on the weathering of PETG and PCTT films. *Journal of Applied Polymer Science*, *136*(47), 48198. https://doi.org/10.1002/app.48198

Atamanalp, M., Köktürk, M., Uçar, A., Duyar, H. A., Özdemir, S., Parlak, V., Esenbuğa, N., & Alak, G. (2021). Microplastics in Tissues (Brain, Gill, Muscle and Gastrointestinal) of Mullus barbatus and Alosa immaculata. *Archives of Environmental Contamination and Toxicology*, *81*(3), 460–469. https://doi.org/10.1007/s00244-021-00885-5

Atugoda, T., Vithanage, M., Wijesekara, H., Bolan, N., Sarmah, A. K., Bank, M. S., You, S., & Ok, Y. S. (2021). Interactions between microplastics, pharmaceuticals and personal care products: Implications for vector transport. *Environment International*, *149*, 106367. https://doi.org/10.1016/j.envint.2020.106367

Bergmann, M. (2022). *Plastic pollution in the Arctic | Nature Reviews Earth & Environment*. https://www.nature.com/articles/s43017-022-00279-8

Biale, G., La Nasa, J., Mattonai, M., Corti, A., Vinciguerra, V., Castelvetro, V., & Modugno, F. (2021). A Systematic Study on the Degradation Products Generated from Artificially Aged Microplastics. *Polymers*, *13*(12), Article 12. https://doi.org/10.3390/polym13121997

Binda, G., Spanu, D., Monticelli, D., Pozzi, A., Bellasi, A., Bettinetti, R., Carnati, S., & Nizzetto, L. (2021). Unfolding the interaction between microplastics and (trace) elements in water: A critical review. *Water Research*, *204*, 117637. https://doi.org/10.1016/j.watres.2021.117637

Botterell, Z. L. R., Beaumont, N., Dorrington, T., Steinke, M., Thompson, R. C., & Lindeque, P. K. (2019). Bioavailability and effects of microplastics on marine zooplankton: A review. *Environmental Pollution*, *245*, 98–110. https://doi.org/10.1016/j.envpol.2018.10.065

Boucher, C., Morin, M., & Bendell, L. I. (2015). The influence of cosmetic microbeads on the sorptive behavior of cadmium and lead within intertidal sediments: A laboratory study. *Regional Studies in Marine Science*, *3*. https://doi.org/10.1016/j.rsma.2015.11.009

Boyd, R. D., Pichaimuthu, S. K., & Cuenat, A. (2011). New approach to inter-technique comparisons for nanoparticle size measurements; using atomic force microscopy, nanoparticle tracking analysis and dynamic light scattering. *Colloids and Surfaces A: Physicochemical and Engineering Aspects*, *1–3*(387), 35–42. https://doi.org/10.1016/j.colsurfa.2011.07.020

Bretas Alvim, C., Mendoza-Roca, J. A., & Bes-Piá, A. (2020). Wastewater treatment plant as microplastics release source – Quantification and identification techniques. *Journal of Environmental Management*, *255*, 109739. https://doi.org/10.1016/j.jenvman.2019.109739

Cai, L., Wang, J., Peng, J., Tan, Z., Zhan, Z., Tan, X., & Chen, Q. (2017). Characteristic of microplastics in the atmospheric fallout from Dongguan city, China: Preliminary research and first evidence. *Environmental Science and Pollution Research*, *24*(32), 24928–24935. https://doi.org/10.1007/s11356-017-0116-x

Canada, H. (2005, January 13). *Page 8: Guidelines for Canadian Drinking Water Quality: Guideline Technical Document – Turbidity* [Research;guidance]. https://www.canada.ca/en/health-canada/services/publications/healthy-living/guidelines-canadian-drinking-water-quality-turbidity/page-8-guidelines-canadian-drinking-water-quality-turbidity.html

Cargnello, M., Gordon, T. R., & Murray, C. B. (2014). Solution-Phase Synthesis of Titanium Dioxide Nanoparticles and Nanocrystals. *Chemical Reviews*, *114*(19), 9319–9345. https://doi.org/10.1021/cr500170p

Carlier, P., Hannachi, H., & Mouvier, G. (1986). The chemistry of carbonyl compounds in the atmosphere—A review. *Atmospheric Environment (1967)*, *20*(11), 2079–2099. https://doi.org/10.1016/0004-6981(86)90304-5

Chamas, A., Moon, H., Zheng, J., Qiu, Y., Tabassum, T., Jang, J. H., Abu-Omar, M., Scott, S. L., & Suh, S. (2020). Degradation Rates of Plastics in the Environment. *ACS Sustainable Chemistry & Engineering*, *8*(9), 3494–3511. https://doi.org/10.1021/acssuschemeng.9b06635

Chen, Fu, Z., Yang, H., & Wang, J. (2020). An overview of analytical methods for detecting microplastics in the atmosphere. *TrAC Trends in Analytical Chemistry*, *130*, 115981. https://doi.org/10.1016/j.trac.2020.115981

Chen, Ouyang, Z.-Y., Qian, C., & Yu, H.-Q. (2018). Induced structural changes of humic acid by exposure of polystyrene microplastics: A spectroscopic insight. *Environmental Pollution*, *233*, 1–7. https://doi.org/10.1016/j.envpol.2017.10.027

Cherniak, S. L., Almuhtaram, H., McKie, M. J., Hermabessiere, L., Yuan, C., Rochman, C. M., & Andrews, R. C. (2022). Conventional and biological treatment for the removal of microplastics from drinking water. *Chemosphere*, *288*, 132587. https://doi.org/10.1016/j.chemosphere.2021.132587

Chowdhury, S., Mazumder, M. A. J., Al-Attas, O., & Husain, T. (2016). Heavy metals in drinking water: Occurrences, implications, and future needs in developing countries. *Science of The Total Environment*, *569–570*, 476–488. https://doi.org/10.1016/j.scitotenv.2016.06.166

Christensen, J., & Linden, K. G. (2003). How particles affect UV light in the UV Disinfection of Unfiltered Drinking Water. *Journal AWWA*, *95*(4), 179–189. https://doi.org/10.1002/j.1551-8833.2003.tb10344.x

Clark, J. (2023). *Introduction to IR Spectra*. https://webspectra.chem.ucla.edu/irintro.html

Coffin, S. (2023). The emergence of microplastics: Charting the path from research to regulations. *Environmental Science: Advances*, *2*(3), 356–367. https://doi.org/10.1039/D2VA00275B

Coles, C. A., & Yong, R. N. (2006). Humic acid preparation, properties and interactions with metals lead and cadmium. *Engineering Geology*, *85*(1), 26–32. https://doi.org/10.1016/j.enggeo.2005.09.024

Contado, C. (2017). Field flow fractionation techniques to explore the “nano-world.” *Analytical and Bioanalytical Chemistry*, *409*(10), 2501–2518. https://doi.org/10.1007/s00216-017-0180-6

Cózar, A., Echevarría, F., González-Gordillo, J. I., Irigoien, X., Úbeda, B., Hernández-León, S., Palma, Á. T., Navarro, S., García-de-Lomas, J., Ruiz, A., Fernández-de-Puelles, M. L., & Duarte, C. M. (2014). Plastic debris in the open ocean. *Proceedings of the National Academy of Sciences*, *111*(28), 10239–10244. https://doi.org/10.1073/pnas.1314705111

Dris, R., Gasperi, J., Mirande, C., Mandin, C., Guerrouache, M., Langlois, V., & Tassin, B. (2017). A first overview of textile fibers, including microplastics, in indoor and outdoor environments. *Environmental Pollution*, *221*, 453–458. https://doi.org/10.1016/j.envpol.2016.12.013

Efimova, I., Bagaeva, M., Bagaev, A., Kileso, A., & Chubarenko, I. P. (2018). Secondary Microplastics Generation in the Sea Swash Zone With Coarse Bottom Sediments: Laboratory Experiments. *Frontiers in Marine Science*, *5*. https://www.frontiersin.org/articles/10.3389/fmars.2018.00313

Enyoh, C. E., Shafea, L., Verla, A. W., Verla, E. N., Qingyue, W., Chowdhury, T., & Paredes, M. (2020). Microplastics Exposure Routes and Toxicity Studies to Ecosystems: An Overview. *Environmental Analysis, Health and Toxicology*, *35*(1), e2020004. https://doi.org/10.5620/eaht.e2020004

Exline, D. (2013). *Comparison of Raman and FTIR Spectroscopy: Advantages and Limitations—Gateway Analytical*. https://gatewayanalytical.com/resources/publications/comparison-raman-and-ftir-spectroscopy-advantages-and-limitations/

Faghihnejad, & Zheng. (2013). Interaction mechanism between hydrophobic and hydrophilic surfaces: Using polystyrene and mica as a model system. *Langmuir : The ACS Journal of Surfaces and Colloids*, *29*(40). https://doi.org/10.1021/la402244h

Fan, C., Huang, Y.-Z., Lin, J.-N., & Li, J. (2022). Microplastic quantification of nylon and polyethylene terephthalate by chromic acid wet oxidation and ultraviolet spectrometry. *Environmental Technology & Innovation*, *28*, 102683. https://doi.org/10.1016/j.eti.2022.102683

Farrell, C., Hassard, F., Jefferson, B., Leziart, T., Nocker, A., & Jarvis, P. (2018). Turbidity composition and the relationship with microbial attachment and UV inactivation efficacy. *Science of The Total Environment*, *624*, 638–647. https://doi.org/10.1016/j.scitotenv.2017.12.173

Fu, Li, Wang, G., Luan, Y., & Dai, W. (2021). Adsorption behavior of organic pollutants on microplastics. *Ecotoxicology and Environmental Safety*, *217*, 112207. https://doi.org/10.1016/j.ecoenv.2021.112207

Fu, Min, J., Jiang, W., Li, Y., & Zhang, W. (2020). Separation, characterization and identification of microplastics and nanoplastics in the environment. *Science of The Total Environment*, *721*, 137561. https://doi.org/10.1016/j.scitotenv.2020.137561

Gewert, B., M. Plassmann, M., & MacLeod, M. (2015). Pathways for degradation of plastic polymers floating in the marine environment. *Environmental Science: Processes & Impacts*, *17*(9), 1513–1521. https://doi.org/10.1039/C5EM00207A

Geyer, R., Jambeck, J. R., & Law, K. L. (2017). Production, use, and fate of all plastics ever made. *Science Advances*, *3*(7), e1700782. https://doi.org/10.1126/sciadv.1700782

Ghernaout, D. (2015). Brownian Motion and Coagulation Process. *American Journal of Environmental Protection*, *4*(5), 1. https://doi.org/10.11648/j.ajeps.s.2015040501.11

Goh, E. G., Xu, X., & McCormick, P. G. (2014). Effect of particle size on the UV absorbance of zinc oxide nanoparticles. *Scripta Materialia*, *78–79*, 49–52. https://doi.org/10.1016/j.scriptamat.2014.01.033

Goldstein, J. I., Newbury, D. E., Michael, J. R., Ritchie, N. W. M., Scott, J. H. J., & Joy, D. C. (2017). *Scanning Electron Microscopy and X-Ray Microanalysis*. Springer.

Gourmelon, G. (2015). Global plastic production rises, recycling lags. *Vital Signs 22 (2015)*, 91-95.

Harley-Nyang, D., Memon, F. A., Jones, N., & Galloway, T. (2022). Investigation and analysis of microplastics in sewage sludge and biosolids: A case study from one wastewater treatment works in the UK. *Science of The Total Environment*, *823*, 153735. https://doi.org/10.1016/j.scitotenv.2022.153735

Hermabessiere, L., Himber, C., Boricaud, B., Kazour, M., Amara, R., Cassone, A.-L., Laurentie, M., Paul-Pont, I., Soudant, P., Dehaut, A., & Duflos, G. (2018). Optimization, performance, and application of a pyrolysis-GC/MS method for the identification of microplastics. *Analytical and Bioanalytical Chemistry*, *410*(25), 6663–6676. https://doi.org/10.1007/s00216-018-1279-0

Hidalgo-Ruz, V., Gutow, L., Thompson, R. C., & Thiel, M. (2012). Microplastics in the Marine Environment: A Review of the Methods Used for Identification and Quantification. *Environmental Science & Technology*, *46*(6), 3060–3075. https://doi.org/10.1021/es2031505

Ho, W. K., Law, C. F. J., Zhang, T., & Leung, K. (2020). Effects of Weathering on the Sorption Behavior and Toxicity of Polystyrene Microplastics in Multi-solute Systems. *Water Research*, *187*, 116419. https://doi.org/10.1016/j.watres.2020.116419

Hofman-Caris, C. H. M., Bäuerlein, P. S., Siegers, W. G., Mintenig, S. M., Messina, R., Dekker, S. C., Bertelkamp, C., Cornelissen, E. R., & Wezel, A. P. van. (2022). Removal of nanoparticles (both inorganic nanoparticles and nanoplastics) in drinking water treatment – coagulation/flocculation/sedimentation, and sand/granular activated carbon filtration. *Environmental Science: Water Research & Technology*, *8*(8), 1675–1686. https://doi.org/10.1039/D2EW00226D

Holmes, L. A., Turner, A., & Thompson, R. C. (2012). Adsorption of trace metals to plastic resin pellets in the marine environment. *Environmental Pollution (Barking, Essex: 1987)*, *160*(1), 42–48. https://doi.org/10.1016/j.envpol.2011.08.052

Huang, Peng, C., Wang, Z., Xiong, X., Bi, Y., Liu, Y., & Li, D. (2021). Spatiotemporal distribution of microplastics in surface water, biofilms, and sediments in the world's largest drinking water diversion project. *Science of The Total Environment*, *789*, 148001. https://doi.org/10.1016/j.scitotenv.2021.148001

Huang, Zemlyanov, D. Y., Diaz-Amaya, S., Salehi, M., Stanciu, L., & Whelton, A. J. (2020). Competitive heavy metal adsorption onto new and aged polyethylene under various drinking water conditions. *Journal of Hazardous Materials*, *385*, 121585. https://doi.org/10.1016/j.jhazmat.2019.121585

Hüffer, T., Weniger, A.-K., & Hofmann, T. (2018). Sorption of organic compounds by aged polystyrene microplastic particles. *Environmental Pollution*, *236*, 218–225. https://doi.org/10.1016/j.envpol.2018.01.022

Huppertsberg, S., & Knepper, T. P. (2018). Instrumental analysis of microplastics—Benefits and challenges. *Analytical and Bioanalytical Chemistry*, *410*(25), 6343–6352. https://doi.org/10.1007/s00216-018-1210-8

Hwang, J., Choi, D., Han, S., Jung, S. Y., Choi, J., & Hong, J. (2020). Potential toxicity of polystyrene microplastic particles. *Scientific Reports*, *10*(1), 7391-. https://doi.org/10.1038/s41598-020-64464-9

ImageJ. (n.d.). ImageJ Wiki. Retrieved February 7, 2023, from https://imagej.github.io/software/imagej/index

Industries, C. (2021, March 5). Polymer Water Treatment: How Coagulants & Flocculants Clean Water. *Clearwater Industries, Inc.* https://clearwaterind.com/polymer-water-treatment-how-coagulants-and-flocculants-clean-wastewater/

Kaiser, D., Kowalski, N., & Waniek, J. J. (2017). Effects of biofouling on the sinking behavior of microplastics. *Environmental Research Letters*, *12*(12), 124003. https://doi.org/10.1088/1748-9326/aa8e8b

Käppler, A., Fischer, D., Oberbeckmann, S., Schernewski, G., Labrenz, M., Eichhorn, K.-J., & Voit, B. (2016). Analysis of environmental microplastics by vibrational microspectroscopy: FTIR, Raman or both? *Analytical and Bioanalytical Chemistry*, *408*(29), 8377–8391. https://doi.org/10.1007/s00216-016-9956-3

Karimi Estahbanati, M. R., Rostami, S., Ghasemian, M., Kiendrebeogo, M., Drogui, P., & Tyagi, R. D. (2023). Chapter 5—Quantitative and qualitative identification, characterization, and analysis of microplastics and nanoplastics in water. In R. D. Tyagi, A. Pandey, P. Drogui, B. Yadav, & S. Pilli (Eds.), *Current Developments in Biotechnology and Bioengineering* (pp. 99–123). Elsevier. https://doi.org/10.1016/B978-0-323-99908-3.00020-8

Kirstein, I. V., Gomiero, A., & Vollertsen, J. (2021). Microplastic pollution in drinking water. *Current Opinion in Toxicology*, *28*, 70–75. https://doi.org/10.1016/j.cotox.2021.09.003

Kirstein, I. V., Hensel, F., Gomiero, A., Iordachescu, L., Vianello, A., Wittgren, H. B., & Vollertsen, J. (2021). Drinking plastics? – Quantification and qualification of microplastics in drinking water distribution systems by μFTIR and Py-GCMS. *Water Research*, *188*, 116519. https://doi.org/10.1016/j.watres.2020.116519

Klein, M., & Fischer, E. K. (2019). Microplastic abundance in atmospheric deposition within the Metropolitan area of Hamburg, Germany. *Science of The Total Environment*, *685*, 96–103. https://doi.org/10.1016/j.scitotenv.2019.05.405

Krishna, R., Chintalpudi, V., & Muddada, S. (2018). *Application of Biosorption for Removal of Heavy Metals from Wastewater*. https://doi.org/10.5772/intechopen.77315

Kurunthachalam, K. (2021). *Frontiers | A Review of Human Exposure to Microplastics and Insights Into Microplastics as Obesogens*. https://www.frontiersin.org/articles/10.3389/fendo.2021.724989/full

Lapointe, M., Farner, J. M., Hernandez, L. M., & Tufenkji, N. (2020). Understanding and Improving Microplastic Removal during Water Treatment: Impact of Coagulation and Flocculation. *Environmental Science & Technology*, *54*(14), 8719–8727. https://doi.org/10.1021/acs.est.0c00712

Leusch, F. D. L., & Ziajahromi, S. (2021). Converting mg/L to Particles/L: Reconciling the Occurrence and Toxicity Literature on Microplastics. *Environmental Science & Technology*, *55*(17), 11470–11472. https://doi.org/10.1021/acs.est.1c04093

Li, Guo, K., Cao, Y., Wang, S., Song, Y., & Zhang, H. (2021). Enhance in mobility of oxytetracycline in a sandy loamy soil caused by the presence of microplastics. *Environmental Pollution*, *269*, 116151. https://doi.org/10.1016/j.envpol.2020.116151

Li, Liu, H., & Paul Chen, J. (2018). Microplastics in freshwater systems: A review on occurrence, environmental effects, and methods for microplastics detection. *Water Research*, *137*, 362–374. https://doi.org/10.1016/j.watres.2017.12.056

Li, T., Zhou, C., & Jiang, M. (n.d.). *9 Springer-Verlag 1991 UV absorption spectra of polystyrene*.

Li, T., Zhou, C., & Jiang, M. (1991). UV absorption spectra of polystyrene. *Polymer Bulletin*, *25*(2), 211–216. https://doi.org/10.1007/BF00310794

Lin, J., Yan, D., Fu, J., Chen, Y., & Ou, H. (2020). Ultraviolet-C and vacuum ultraviolet inducing surface degradation of microplastics. *Water Research*, *186*, 116360. https://doi.org/10.1016/j.watres.2020.116360

Liu, Shi, J., Wang, J., Dai, Y., Li, H., Li, J., Liu, X., Chen, X., Wang, Z., & Zhang, P. (2021). Interactions Between Microplastics and Heavy Metals in Aquatic Environments: A Review. *Frontiers in Microbiology*, *12*.

https://www.frontiersin.org/article/10.3389/fmicb.2021.652520

Liu, Wu, T., Wang, X., Song, Z., Zong, C., Wei, N., & Li, D. (2019). Consistent Transport of Terrestrial Microplastics to the Ocean through Atmosphere. *Environmental Science & Technology*, *53*(18), 10612–10619. https://doi.org/10.1021/acs.est.9b03427

Löder, M. G. J., & Gerdts, G. (2015). Methodology Used for the Detection and Identification of Microplastics—A Critical Appraisal. In M. Bergmann, L. Gutow, & M. Klages (Eds.), *Marine Anthropogenic Litter* (pp. 201–227). Springer International Publishing. https://doi.org/10.1007/978-3-319-16510-3_8

Luo, X., Wang, Z., Yang, L., Gao, T., & Zhang, Y. (2022). A review of analytical methods and models used in atmospheric microplastic research. *Science of The Total Environment*, *828*, 154487. https://doi.org/10.1016/j.scitotenv.2022.154487

Malatesta, M. (2021). Transmission Electron Microscopy as a Powerful Tool to Investigate the Interaction of Nanoparticles with Subcellular Structures. *International Journal of Molecular Sciences*, *22*(23), 12789. https://doi.org/10.3390/ijms222312789

Manceau, A., Boisset, M.-C., Sarret, G., Hazemann, J.-L., Mench, M., Cambier, P., & Prost, R. (1996). Direct Determination of Lead Speciation in Contaminated Soils by EXAFS Spectroscopy. *Environmental Science & Technology*, *30*(5), 1540–1552. https://doi.org/10.1021/es9505154

Mani, T., Hauk, A., Walter, U., & Burkhardt-Holm, P. (2015). Microplastics profile along the Rhine River. *Scientific Reports*, *5*, 17988. https://doi.org/10.1038/srep17988

Mason, S. A., Garneau, D., Sutton, R., Chu, Y., Ehmann, K., Barnes, J., Fink, P., Papazissimos, D., & Rogers, D. L. (2016). Microplastic pollution is widely detected in US municipal wastewater treatment plant effluent. *Environmental Pollution*, *218*, 1045–1054. https://doi.org/10.1016/j.envpol.2016.08.056

Mattsson, K., Björkroth, F., Karlsson, T., & Hassellöv, M. (2021). Nanofragmentation of Expanded Polystyrene Under Simulated Environmental Weathering (Thermooxidative Degradation and Hydrodynamic Turbulence). *Frontiers in Marine Science*, *7*. https://www.frontiersin.org/articles/10.3389/fmars.2020.578178

Mausra, B., & Foster, A. (n.d.). *Laboratory Methods for the Analysis of Microplastics in the Marine Environment*. 39.

Mendez, D., Rodriguez, E., Acosta Coley, I., Rosa, J., & Olivero-Verbel, J. (2019). Trace elements in microplastics in Cartagena: A hotspot for plastic pollution at the Caribbean. *Marine Pollution Bulletin*, *139*, 402–411. https://doi.org/10.1016/j.marpolbul.2018.12.016

Mintenig, S. M., Bäuerlein, P. S., Koelmans, A. A., Dekker, S. C., & van Wezel, A. P. (2018). Closing the gap between small and smaller: Towards a framework to analyse nano- and microplastics in aqueous environmental samples. *Environmental Science: Nano*, *5*(7), 1640–1649. https://doi.org/10.1039/C8EN00186C

Mintenig, S. M., Int-Veen, I., Löder, M. G. J., Primpke, S., & Gerdts, G. (2017). Identification of microplastic in effluents of waste water treatment plants using focal plane array-based micro-Fourier-transform infrared imaging. *Water Research*, *108*, 365–372. https://doi.org/10.1016/j.watres.2016.11.015

Möller, J. N., Löder, M. G. J., & Laforsch, C. (2020). Finding Microplastics in Soils: A Review of Analytical Methods. *Environmental Science & Technology*, *54*(4), 2078–2090. https://doi.org/10.1021/acs.est.9b04618

Munoz, M., Ortiz, D., Nieto-Sandoval, J., de Pedro, Z. M., & Casas, J. A. (2021). Adsorption of micropollutants onto realistic microplastics: Role of microplastic nature, size, age, and NOM fouling. *Chemosphere*, *283*, 131085. https://doi.org/10.1016/j.chemosphere.2021.131085

Ngo, P. L., Pramanik, B. K., Shah, K., & Roychand, R. (2019). Pathway, classification and removal efficiency of microplastics in wastewater treatment plants. *Environmental Pollution (Barking, Essex: 1987)*, *255*(Pt 2), 113326. https://doi.org/10.1016/j.envpol.2019.113326

Nguyen, T.-B., Ho, T.-B.-C., Huang, C. P., Chen, C.-W., Chen, W.-H., Hsieh, S., Hsieh, S.-L., & Dong, C.-D. (2022). Adsorption of lead(II) onto PE microplastics as a function of particle size: Influencing factors and adsorption mechanism. *Chemosphere*, *304*, 135276. https://doi.org/10.1016/j.chemosphere.2022.135276

Nurmukhametov, R. N., Volkova, L. V., & Kabanov, S. P. (2006). Fluorescence and absorption of polystyrene exposed to UV laser radiation. *Journal of Applied Spectroscopy*, *73*(1), 55–60. https://doi.org/10.1007/s10812-006-0035-y

Okada, T. (2007). PARTICLE SIZE SEPARATION | Field Flow Fractionation: Electric Fields. In I. D. Wilson (Ed.), *Encyclopedia of Separation Science* (pp. 1–6). Academic Press. https://doi.org/10.1016/B0-12-226770-2/07001-0

Omidi, M., Fatehinya, A., Farahani, M., Akbari, Z., Shahmoradi, S., Yazdian, F., Tahriri, M., Moharamzadeh, K., Tayebi, L., & Vashaee, D. (2017). 7—Characterization of biomaterials. In L. Tayebi & K. Moharamzadeh (Eds.), *Biomaterials for Oral and Dental Tissue Engineering* (pp. 97–115). Woodhead Publishing. https://doi.org/10.1016/B978-0-08-100961-1.00007-4

Osorio, E., Tanchuling, M., & Diola, Ma. B. L. (2021). Microplastics Occurrence in Surface Waters and Sediments in Five River Mouths of Manila Bay. *Frontiers in Environmental Science*, *9*. https://doi.org/10.3389/fenvs.2021.719274

Patil, M. (2020, April 4). Chrominfo: Advantages and disadvantages of size exclusion chromatography. *Chrominfo*. https://chrominfo.blogspot.com/2020/04/advantages-and-disadvantages-of-size.html

Peller, J. R., Nelson, C. R., Babu, B. G., Iceman, C., & Kostelnik, E. (2020). A Review of Microplastics in Freshwater Environments: Locations, Methods, and Pollution Loads. In *Contaminants in Our Water: Identification and Remediation Methods* (Vol. 1352, pp. 65–90). American Chemical Society. https://doi.org/10.1021/bk-2020-1352.ch004

Peters, C. A., Hendrickson, E., Minor, E. C., Schreiner, K., Halbur, J., & Bratton, S. P. (2018). Pyr-GC/MS analysis of microplastics extracted from the stomach content of benthivore fish from the Texas Gulf Coast. *Marine Pollution Bulletin*, *137*, 91–95. https://doi.org/10.1016/j.marpolbul.2018.09.049

Pivokonsky, M., Cermakova, L., Novotna, K., Peer, P., Cajthaml, T., & Janda, V. (2018). Occurrence of microplastics in raw and treated drinking water. *Science of The Total Environment*, *643*, 1644–1651. https://doi.org/10.1016/j.scitotenv.2018.08.102

Prata, J. C., Castro, J. L., da Costa, J. P., Duarte, A. C., Cerqueira, M., & Rocha-Santos, T. (2020). An easy method for processing and identification of natural and synthetic microfibers and microplastics in indoor and outdoor air. *MethodsX*, *7*, 100762. https://doi.org/10.1016/j.mex.2019.11.032

Quinn, B., Murphy, F., & Ewins, C. (2017). Validation of density separation for the rapid recovery of microplastics from sediment. *Analytical Methods*, *9*(9), 1491–1498. https://doi.org/10.1039/C6AY02542K

Sarkar, A. K., Rubin, A. E., & Zucker, I. (2021). Engineered Polystyrene-Based Microplastics of High Environmental Relevance. *Environmental Science & Technology*, *55*(15), 10491–10501. https://doi.org/10.1021/acs.est.1c02196

Schernewski, G., Radtke, H., Hauk, R., Baresel, C., Olshammar, M., Osinski, R., & Oberbeckmann, S. (2020). Transport and Behavior of Microplastics Emissions From Urban Sources in the Baltic Sea. *Frontiers in Environmental Science*, *0*. https://doi.org/10.3389/fenvs.2020.579361

Semcesen, P. O., & Wells, M. G. (2021). Biofilm growth on buoyant microplastics leads to changes in settling rates: Implications for microplastic retention in the Great Lakes. *Marine Pollution Bulletin*, *170*, 112573. https://doi.org/10.1016/j.marpolbul.2021.112573

Shen, M., Song, B., Zeng, G., Zhang, Y., Teng, F., & Zhou, C. (2021). Surfactant changes lead adsorption behaviors and mechanisms on microplastics. *Chemical Engineering Journal*, *405*, 126989. https://doi.org/10.1016/j.cej.2020.126989

Smith, M. (2018). *Microplastics in Seafood and the Implications for Human Health | SpringerLink*. https://link.springer.com/article/10.1007/s40572-018-0206-z

Song, Y. K., Hong, S. H., Jang, M., Han, G. M., Jung, S. W., & Shim, W. J. (2017). Combined Effects of UV Exposure Duration and Mechanical Abrasion on Microplastic Fragmentation by Polymer Type. *Environmental Science & Technology*, *51*(8), 4368–4376. https://doi.org/10.1021/acs.est.6b06155

Stetefeld, J., McKenna, S. A., & Patel, T. R. (2016). Dynamic light scattering: A practical guide and applications in biomedical sciences. *Biophysical Reviews*, *8*(4), 409–427. https://doi.org/10.1007/s12551-016-0218-6

Sun, Chen, B., Li, Q., Liu, N., Xia, B., Zhu, L., & Qu, K. (2018). Toxicities of polystyrene nano- and microplastics toward marine bacterium Halomonas alkaliphila. *Science of The Total Environment*, *642*, 1378–1385. https://doi.org/10.1016/j.scitotenv.2018.06.141

Sun, H., Jiao, R., Xu, H., An, G., & Wang, D. (2019). The influence of particle size and concentration combined with pH on coagulation mechanisms. *Journal of Environmental Sciences*, *82*, 39–46. https://doi.org/10.1016/j.jes.2019.02.021

Talvitie, J., Mikola, A., Koistinen, A., & Setälä, O. (2017). Solutions to microplastic pollution—Removal of microplastics from wastewater effluent with advanced wastewater treatment technologies. *Water Research*, *123*, 401–407. https://doi.org/10.1016/j.watres.2017.07.005

Tofa, T. S., Kunjali, K. L., Paul, S., & Dutta, J. (2019). Visible light photocatalytic degradation of microplastic residues with zinc oxide nanorods. *Environmental Chemistry Letters*, *17*(3), 1341–1346. https://doi.org/10.1007/s10311-019-00859-z

Tom, J. (2021). *UV-Vis Spectroscopy: Principle, Strengths and Limitations and Applications | Technology Networks*. https://www.technologynetworks.com/analysis/articles/uv-vis-spectroscopy-principle-strengths-and-limitations-and-applications-349865

Troester, M., Brauch, H.-J., & Hofmann, T. (2016). Vulnerability of drinking water supplies to engineered nanoparticles. *Water Research*, *96*, 255–279. https://doi.org/10.1016/j.watres.2016.03.038

Tsuchiya, T. (2018). Van der Waals Force. In W. M. White (Ed.), *Encyclopedia of Geochemistry: A Comprehensive Reference Source on the Chemistry of the Earth* (pp. 1473–1474). Springer International Publishing. https://doi.org/10.1007/978-3-319-39312-4_329

Ville, M. (2015). *A comparison of rheology and FTIR in the study of polypropylene and polystyrene photodegradation—Mylläri—2015—Journal of Applied Polymer Science—Wiley Online Library*. https://onlinelibrary.wiley.com/doi/full/10.1002/app.42246

Vladilo, G., & Hassanali, A. (2018). Hydrogen Bonds and Life in the Universe. *Life*, *8*(1), 1. https://doi.org/10.3390/life8010001

Wagner, M., Scherer, C., Alvarez-Muñoz, D., Brennholt, N., Bourrain, X., Buchinger, S., Fries, E., Grosbois, C., Klasmeier, J., Marti, T., Rodriguez-Mozaz, S., Urbatzka, R., Vethaak, A. D., Winther-Nielsen, M., & Reifferscheid, G. (2014). Microplastics in freshwater ecosystems: What we know and what we need to know. *Environmental Sciences Europe*, *26*(1), 12. https://doi.org/10.1186/s12302-014-0012-7

Wang, Ndungu, A. W., Li, Z., & Wang, J. (2017). Microplastics pollution in inland freshwaters of China: A case study in urban surface waters of Wuhan, China. *Science of The Total Environment*, *575*, 1369–1374. https://doi.org/10.1016/j.scitotenv.2016.09.213

Wang, & Wang, J. (2018). Investigation of microplastics in aquatic environments: An overview of the methods used, from field sampling to laboratory analysis. *TrAC Trends in Analytical Chemistry*, *108*, 195–202. https://doi.org/10.1016/j.trac.2018.08.026

Wang, Wang, P., Wang, C., & Ao, Y. (2019). Effects of interactions between humic acid and heavy metal ions on the aggregation of TiO2 nanoparticles in water environment. *Environmental Pollution*, *248*, 834–844. https://doi.org/10.1016/j.envpol.2019.02.084

Wilkinson, K. J., Negre, J.-C., & Buffle, J. (1997). Coagulation of colloidal material in surface waters: The role of natural organic matter. *Journal of Contaminant Hydrology*, *26*(1), 229–243. https://doi.org/10.1016/S0169-7722(96)00071-X

Wu, P., Huang, J., Zheng, Y., Yang, Y., Zhang, Y., He, F., Chen, H., Quan, G., Yan, J., Li, T., & Gao, B. (2019). Environmental occurrences, fate, and impacts of microplastics. *Ecotoxicology and Environmental Safety*, *184*, 109612. https://doi.org/10.1016/j.ecoenv.2019.109612

Yousif, E., & Haddad, R. (2013). Photodegradation and photostabilization of polymers, especially polystyrene: Review. *SpringerPlus*, *2*, 398. https://doi.org/10.1186/2193-1801-2-398

Yu, H., Zhang, Y., Tan, W., & Zhang, Z. (2022). Microplastics as an Emerging Environmental Pollutant in Agricultural Soils: Effects on Ecosystems and Human Health. *Frontiers in Environmental Science*, *10*. https://www.frontiersin.org/articles/10.3389/fenvs.2022.855292

Zhang, Cheng, Wang, Y., Duan, Z., Cui, W., Shi, Y., & Qin, L. (2022). Influence of Functional Group Modification on the Toxicity of Nanoplastics. *Frontiers in Marine Science*, *8*. https://www.frontiersin.org/articles/10.3389/fmars.2021.800782

Zhang, Diehl, A., Lewandowski, A., Gopalakrishnan, K., & Baker, T. (2020a). Removal Efficiency of Micro- and Nanoplastics (180 nm – 125 μm) During Drinking Water Treatment. *The Science of the Total Environment*, *720*, 137383. https://doi.org/10.1016/j.scitotenv.2020.137383

Zhang, Diehl, A., Lewandowski, A., Gopalakrishnan, K., & Baker, T. (2020b). Removal efficiency of micro- and nanoplastics (180 nm–125 μm) during drinking water treatment. *Science of The Total Environment*, *720*, 137383. https://doi.org/10.1016/j.scitotenv.2020.137383

Zhang, Jiang, H., Bian, K., Wang, H., & Wang, C. (2021). A critical review of control and removal strategies for microplastics from aquatic environments. *Journal of Environmental Chemical Engineering*, *9*(4), 105463. https://doi.org/10.1016/j.jece.2021.105463

Zhang, Wang, Zhou, Zhou, Dai, Zhou, Q., Chriestie, P., & Luo, Y. (2018). Enhanced adsorption of oxytetracycline to weathered microplastic polystyrene: Kinetics, isotherms and influencing factors. *Environmental Pollution*, *243*, 1550–1557. https://doi.org/10.1016/j.envpol.2018.09.122

Zhang, Zhu, Yang, B., Jia, F., Yan, H., Zeng, M., & Qu, H. (2019). EFFECT of Pb2+ on the flotation of molybdenite in the presence of sulfide ion. *Results in Physics*, *14*, 102361. https://doi.org/10.1016/j.rinp.2019.102361

Zhao, X., Jia, Q., Song, N., Zhou, W., & Li, Y. (2010). Adsorption of Pb(II) from an Aqueous Solution by Titanium Dioxide/Carbon Nanotube Nanocomposites: Kinetics, Thermodynamics, and Isotherms. *Journal of Chemical & Engineering Data*, *55*(10), 4428–4433. https://doi.org/10.1021/je100586r

Zhu, X., Qiang, L., Shi, H., & Cheng, J. (2020). Bioaccumulation of microplastics and its in vivo interactions with trace metals in edible oysters. *Marine Pollution Bulletin*, *154*, 111079. https://doi.org/10.1016/j.marpolbul.2020.111079

Ziajahromi, S., Neale, P. A., Telles Silveira, I., Chua, A., & Leusch, F. D. L. (2021). An audit of microplastic abundance throughout three Australian wastewater treatment plants. *Chemosphere*, *263*, 128294. https://doi.org/10.1016/j.chemosphere.2020.128294

Appendix A Supplementary Information

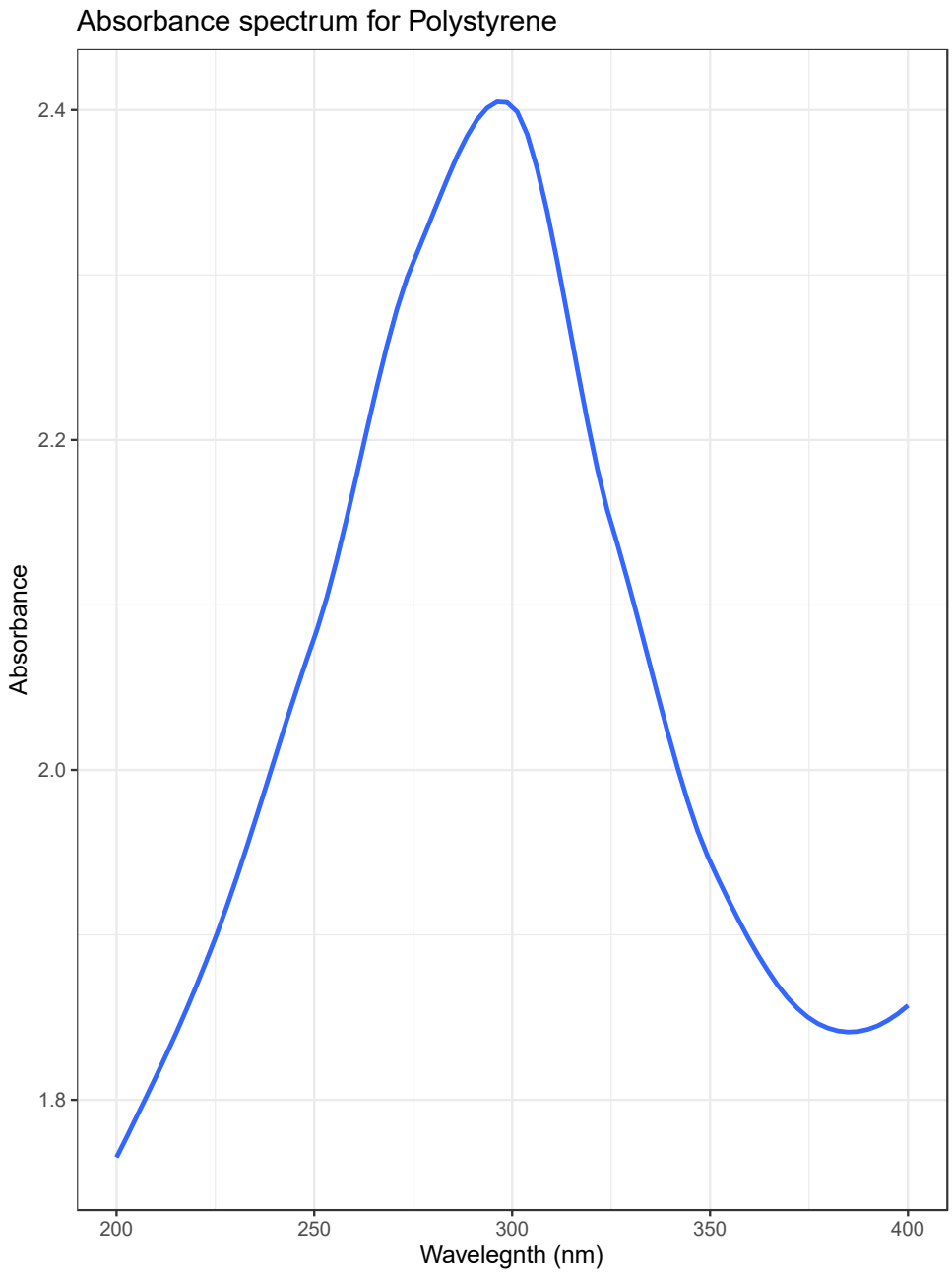

Figure A.1 *Wavelegnth spectra for 0.3um polystyrene beads*

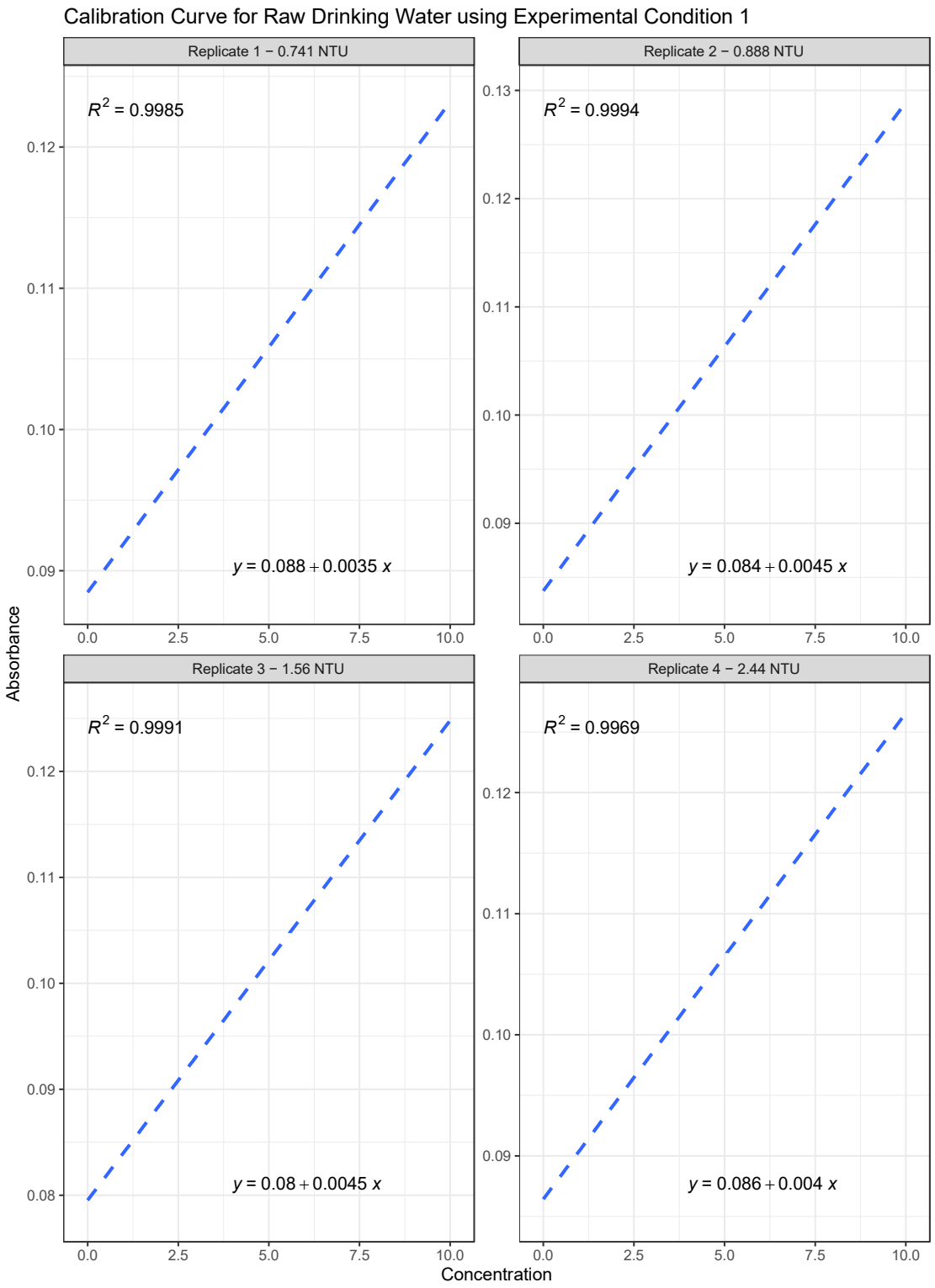

Figure A.2 *Raw drinking water calibration curves for varying influent turbidities for recovery percent calculations.*

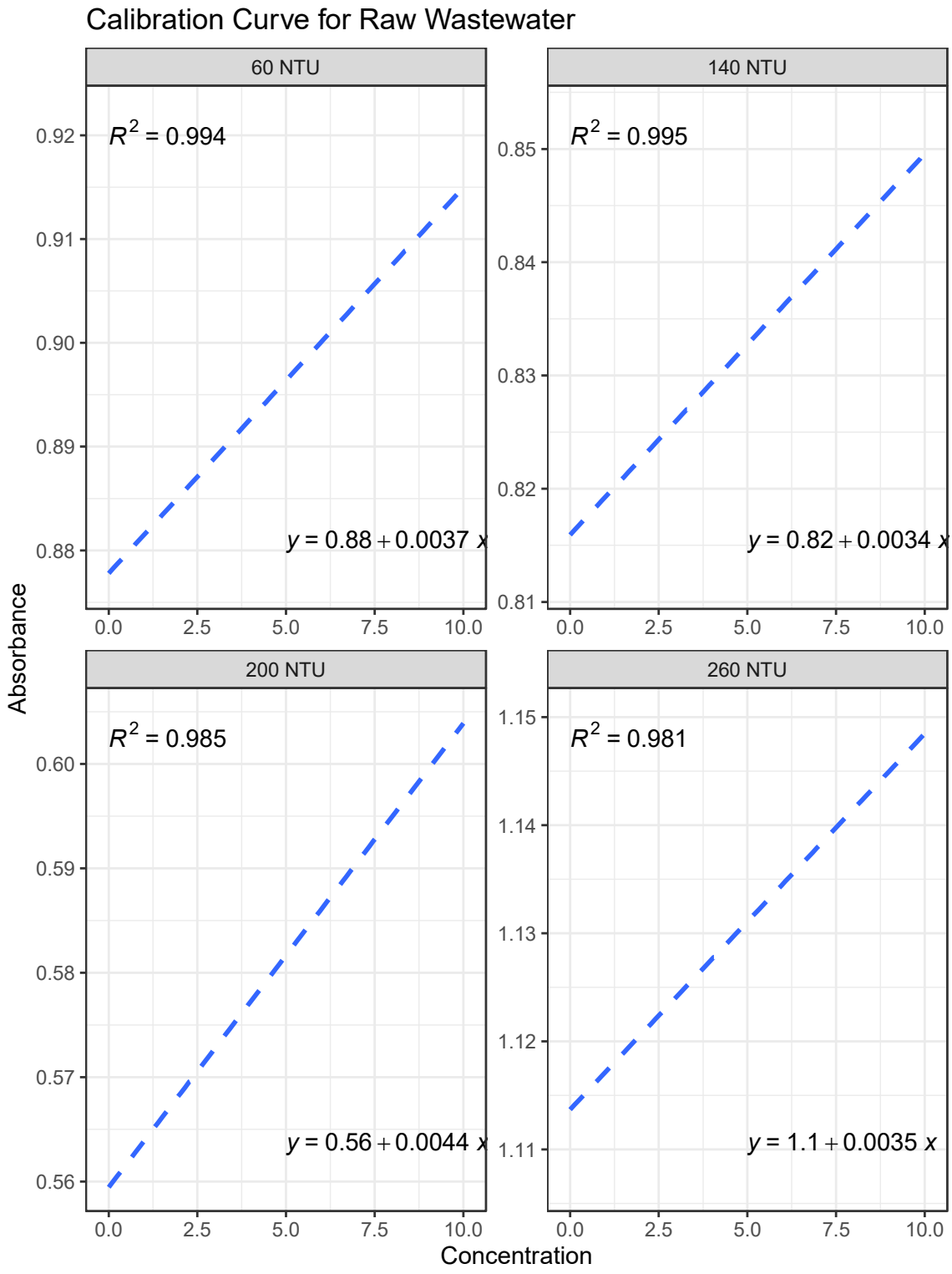

Figure A.3 *Raw wastewater calibration curves for varying influent turbidities for recovery percent calculations.*

Recovery Quality Control

The recovery percent of the method used is dependent on the calibration of the initial turbidity of the influent. For samples having influent turbidity > 0.888 NTU the recovery was 99%. This was calculated by determining the variance between the known spiked value of 10mg/L and the calculated value using the slope equation using the raw water calibration curve. As initial influent turbidity increased from 0.888 NTU up 140 NTU, observed within wastewater samples, the recovery of the method decreased to 97%. At levels higher than 140 NTU the level of recovery for this proposed method dropped to 92% for all remaining samples. This decrease can be further illustrated by the decrease in r^2 values showing that calibration is more effective on samples having lower turbidities. Since all final treated sample turbidity levels were well below 140 NTU, the method used is valid for all samples.

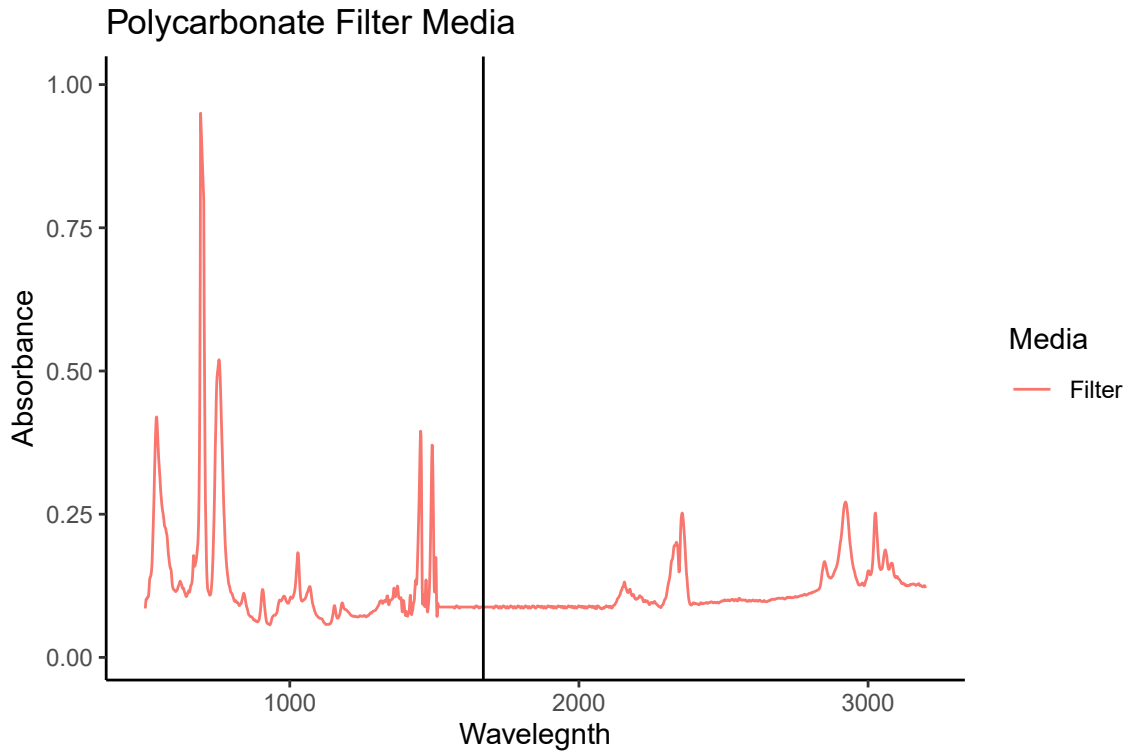

Figure A.4 *Polycarbonate FTIR spectra with band at 1670 to show significant peaks are present*

Table A.1 *Zeta potential values of PS microplastics before and after irradiation*

Irradiance (mJ/cm2)	**Zeta Potential**	
	Initial	Final
0	-37.34	-36.84
180	-36.41	-36.68
1080	-37.11	-37.40
3060	-37.18	-36.93

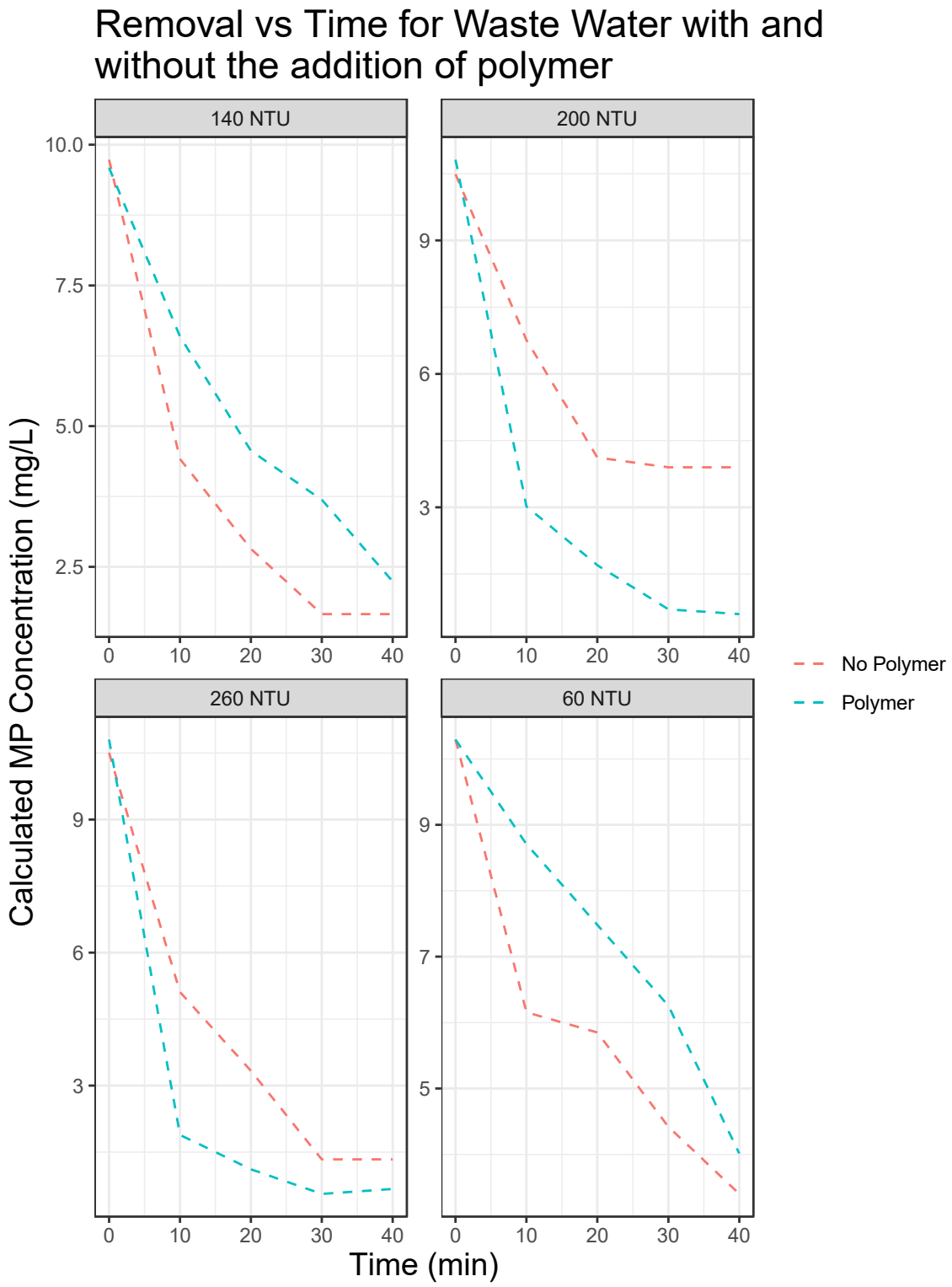

Figure A.5 *Removal vs Time of wastewater samples at increasing turbidites with and without the addition of cationic polymer*

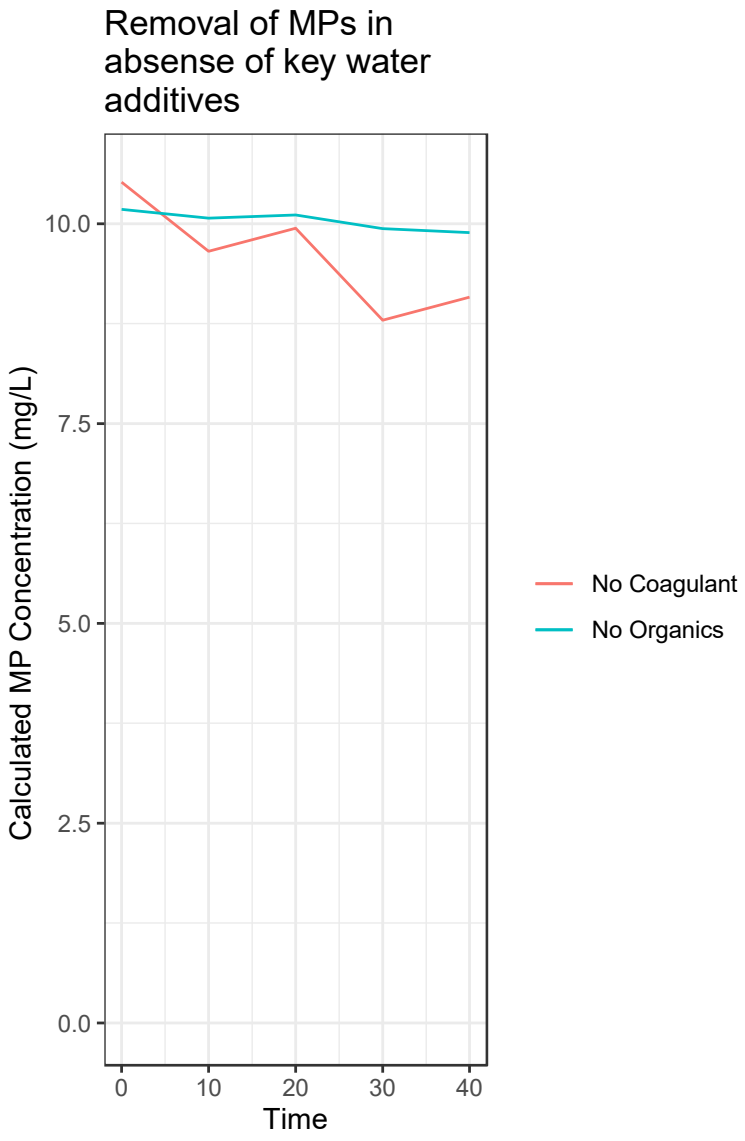

Figure A.6 *Removal vs Time of PS microplastics in the absence of organics as well as coagulant*